Research Paper

Discovery and identification of the prognostic significance and potential mechanism of FMO2 in breast cancer

Lichun Wu[1,*], Jie Chu[2,*], Lijuan Shangguan[3], Mingfei Cao[4], Feng Lu[5]

[1]Department of Clinical Laboratory, Sichuan Cancer Hospital and Institute, Sichuan Cancer Center, School of Medicine, University of Electronic Science and Technology of China, Chengdu, China
[2]The First People's Hospital of Ziyang, Ziyang, China
[3]Outpatient Department, People's Hospital of Jianyang, Jianyang, China
[4]Department of Clinical Laboratory, Chuankong Hospital of Jianyang, Jianyang, China
[5]Department of Experimental Medicine, The People's Hospital of Jianyang City, Jianyang, China
*Equal contribution

Correspondence to: Feng Lu; **email:** lufeng22@126.com, https://orcid.org/0000-0002-7044-6134
Keywords: breast cancer, FMO2, SFRP1, prognosis prediction, predictive biomarker
Received: July 4, 2023 **Accepted:** October 3, 2023 **Published:** November 13, 2023

ABSTRACT

Background: Flavin containing dimethylaniline monoxygenase 2 (FMO2), is downexpressed in diverse tumors and displays vital roles in tumorigenesis. However, the prognostic value and potential mechanism of FMO2 in breast cancer remain unclear.

Methods: The expression of FMO2 was analyzed and the relationship between FMO2 expression level and clinical indicators in breast cancer was analyzed. Then the prognostic value of FMO2 in breast cancer was assessed. The FMO2-correlated genes were obtained, and the highest-ranked gene was chosen. The expression, therapeutic responder analysis, and gene set enrichment analysis of the highest-ranked gene were conducted.

Results: FMO2 was downregulated in breast cancer and was closely related to clinical indicators. Patients with decreased FMO2 expression showed poor overall survival, post-progression survival, relapse-free survival, and distant metastasis-free survival. FMO2 correlates with N/ER/PR subgroups in breast cancer and patients with high FMO2 levels were sensitive to anti-programmed cell death protein 1, anti-programmed death-ligand 1, and anti-cytotoxic T-lymphocyte antigen 4 immunotherapies. Mechanically, FMO2 was positively and highly correlated with secreted Frizzled-related protein 1 (SFRP1), which was downregulated in breast cancer due to hypermethylation. Moreover, SFRP1 was correlated to pathological complete response and relapse-free survival status at 5 years regardless of any chemotherapy, hormone therapy, and anti-HER2 therapy. Gene set enrichment analysis revealed enrichment of component and coagulation cascades, focal adhesion, protein export, and spliceosome.

Conclusions: FMO2 was lower expressed in breast cancer than normal tissues and contributes to subtype classification and prognosis prediction with co-expressed SFRP1.

INTRODUCTION

Breast cancer has surpassed lung cancer as the most common cancer diagnosed, with an estimated increase of 2.3 million cases [1]. Breast cancer accounts for 25% of cancers in women worldwide [2], and it is also the number one cause of cancer-related deaths among women in the world [3, 4]. Compared with transitioned

countries, the mortality rate of breast cancer in transitioning countries is much higher [1]. Although some studies have shown that clinical, pathological indicators and molecular indicators can predict the prognosis of breast cancer [5, 6], early detection, clinical staging, management decision-making and direct treatment of breast cancer are all crucial to the clinical prognosis [7].

Flavin containing dimethylaniline monoxygenase 2 (FMO2), one of the FMO family, is an NADPH-dependent enzyme that catalyzes the N-oxidation of some primary alkylamines through an N-hydroxylamine intermediate [8]. FMO2 prevents cardiac fibrosis via CYP2J3-SMURF2 axis [9], cancer-associated fibroblasts-derived FMO2 acts as a biomarker of macrophage infiltration and prognosis in epithelial ovarian cancer [10]. Although FMO2 is reported to be differentially expressed in tumors, such as early-stage oral squamous cell carcinoma [11], the functional role of FMO2 in breast cancer is largely unknown. Therefore, in the present study, we evaluated the FMO2 expression and its prognostic potential and immunotherapeutic response in breast cancer by comprehensive bioinformatics analysis. In addition, we excavated secreted Frizzled-related protein 1 (SFRP1), a known negative regulator of the Wnt/β-catenin pathway [12], from the perspective of co-expression analysis to reveal the potential molecular mechanism of FMO2 in breast cancer.

MATERIALS AND METHODS

FMO2 expression in breast cancer

The FMO2 mRNA expression level was analyzed across all tissues in all available normal and tumor RNA Seq data from Genotype-Tissue Expression (GTEx), The Cancer Genome Atlas (TCGA), and Therapeutically Applicable Research to Generate Effective Treatments (TARGET) through TNMplot [13]. Then the transcript per million of FMO2 was validated in breast invasive carcinoma through UALCAN [14].

FMO2 expression and different clinical indicators in breast cancer

The expression of FMO2 in different subtypes of breast cancer according to the clinical indicators, including estrogen receptor (ER) status, progesterone receptor (PR) status, human epidermal growth factor receptor 2 (HER2) status, histological types, pathological tumor stage, age status, PAM50 subtypes, triple-negative breast cancer, Ki67 status, Scarff Bloom and Richardson grade status, and Nottingham Prognostic Index status, was analyzed in TCGA (743 breast cancer patients and 92 normal control) and Sweden Cancerome Analysis Network - Breast (SCAN-B) Initiative [15, 16] (3678 breast cancer patients) through Breast Cancer Gene-Expression Miner (bc-GenExMiner) [17].

Survival analysis

The prognostic value of FMO2 in breast cancer was assessed according to overall survival (OS), post-progression survival (PPS), relapse-free survival (RFS), progression-free survival (PFS), and distant metastasis-free survival (DMFS) using Kaplan–Meier plotter [18], which includes gene chip [19], RNA-sequence [19], protein [20], and immunotherapy [21] from Gene Expression Omnibus, European Genome-Phenome Archive (EGA), and TCGA. Later, the prognostic value of FMO2 in breast cancer was assessed according to OS and DFS among node (N), ER, and PR subgroups in bc-GenExMiner [17] with the TCGA and SCAN-B data. According to FMO2 expression, all patients were divided into high- or low-expression groups, and hazard ratio (HR) with 95% confidence intervals and log-rank P were statistically calculated.

Correlation analysis

The genes that shared positive and negative correlations with FMO2 in breast cancer were obtained from TNMplot [13] with gene chip data and RNA-sequence data [19]. We then obtained the intersection genes of positive correlation and negative correlation with FMO2 through the Venn diagram, as described previously [22–24], and selected the highest-ranked gene for subsequent analysis. The expression correlation between FMO2 and the highest-ranked gene was verified by bc-GenExMiner [17] with breast cancer DNA microarrays data and RNA-sequence data and UCSC Xena [25] with TCGA breast cancer data. Finally, a density plot was used to show the expression level of two genes in different tissues (normal, tumor, and metastatic tissues).

SFRP1 expression in breast cancer

The SFRP1 mRNA expression level was analyzed in pan-cancer through TNMplot [13]. And SFRP1 expression in different tissues (normal, tumor, and metastatic tissues) was analyzed. Finally, the SFRP1 mRNA and protein expression levels were validated through UALCAN [14]. The SFRP1 promoter methylation profile was also calculated.

Therapeutic responder analysis

Subsequently, we used the transcriptomic data of 3104 breast cancer patients to verify the predictive biomarker value of SFRP1 for chemotherapy, hormone therapy, and

anti-HER2 therapy through ROCplot [26]. Response to therapy was determined using either author-reported pathological complete response data or relapse-free survival status at 5 years. SFRP1 expression and therapy response are compared using receiver operating characteristics and Mann-Whitney tests.

Functional analysis

We conducted gene set enrichment analysis (GSEA) with TCGA breast cancer data by LinkedOmics [27] to reduce redundant efforts and focus on the discovery and interpretation of attribute associations.

Availability of data and materials

All data generated or analyzed during this study are included in this published article and its Supplementary Information Files.

RESULTS

FMO2 is downregulated in breast cancer

The pan-cancer analysis indicated FMO2 is dysregulated in various cancers (Figure 1A), including breast cancer. Then TCGA database including 1097 breast invasive

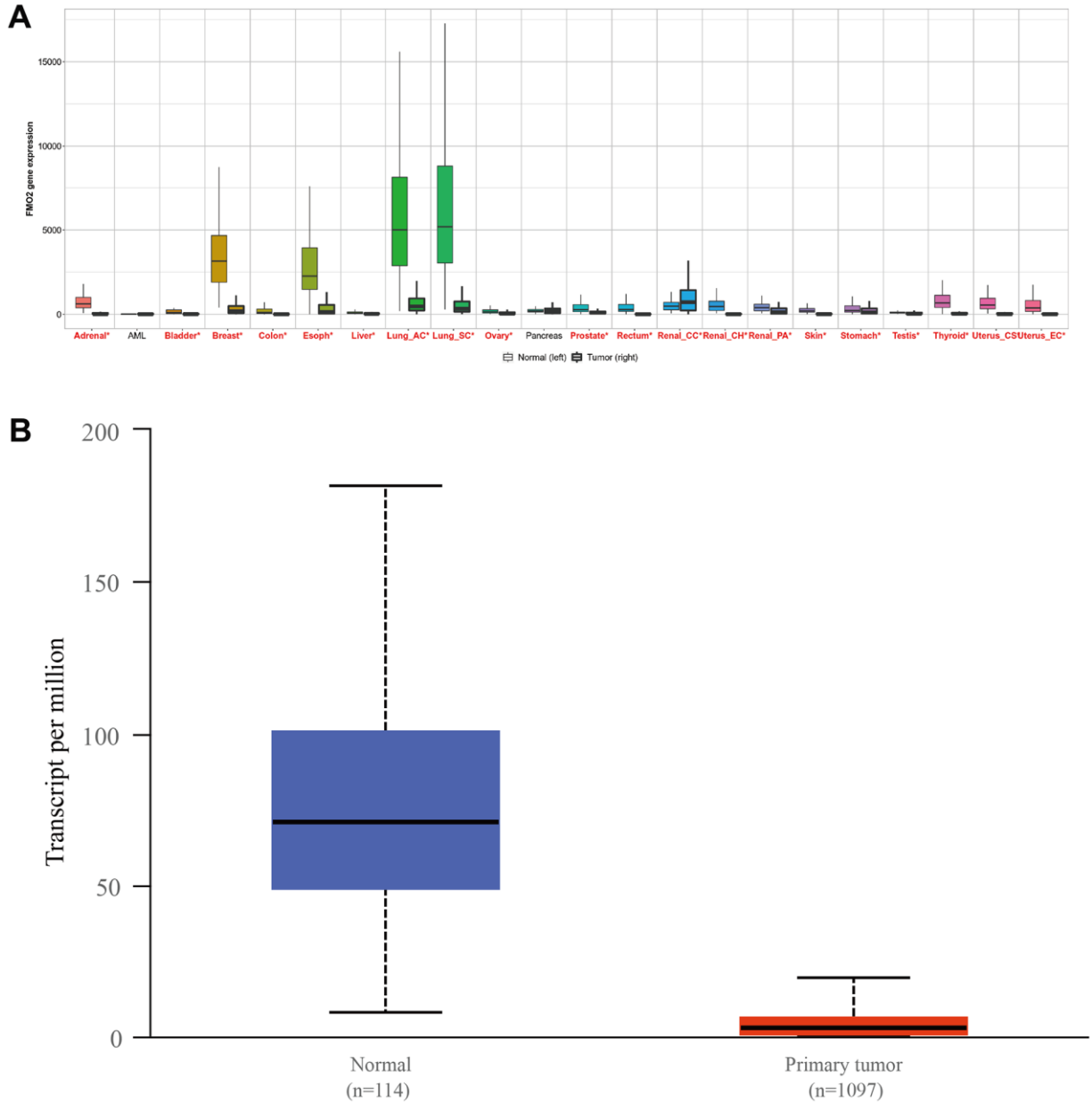

Figure 1. The expression of FMO2 in pan-cancer (**A**) and breast invasive carcinoma, (**B**) P<0.0001.

carcinoma patients and 114 normal patients showed FMO2 is indeed dysregulated (P < 0.0001) (Figure 1B).

The relationship between FMO2 expression and clinical indicators in breast cancer

We next compared FMO2 expression in different subtypes of breast cancer according to different clinical indicators. In the TCGA database, FMO2 was downregulated in breast cancer compared to healthy and tumor-adjacent (P < 0.0001) (Figure 2A and Supplementary Table 1). FMO2 was upregulated in ER- and PR- breast cancer compared to those positive (P < 0.0001 and = 0.0106, respectively) (Figure 2B, 2C and Supplementary Table 1). Similarly, FMO2 was upregulated in ER-/PR- breast cancer (P = 0.0002) (Figure 2D and Supplementary Table 1). FMO2 was downregulated in HER2+ breast cancer (P < 0.0001) (Figure 2E and Supplementary Table 1), mucinous histological type (P < 0.0001) (Figure 2F and Supplementary Table 1), and pathological tumor stage II (P = 0.0067) (Figure 2G and Supplementary Table 1). Patients with age less than 51 years old had higher FMO2 expression (P = 0.0005) (Figure 2H and Supplementary Table 1). FMO2 was also dysregulated in PAM50 subtypes (P < 0.0001) (Figure 2I and Supplementary Table 1). FMO2 was upregulated in basal-like (PAM50) (P < 0.0001) (Figure 2J and Supplementary Table 1), triple-negative breast cancer (P < 0.0001) (Figure 2K and Supplementary Table 1), and basal-like and triple-negative breast cancer (P < 0.0001) (Figure 2L and Supplementary Table 1).

In SCAN-B, FMO2 was upregulated in ER-, PR-, and ER-/PR- breast cancer (P < 0.0001, = 0.0006, and < 0.0001, respectively) (Supplementary Figure 1A–1C and Supplementary Table 1), which was consistent with TCGA. In addition, the expression of FMO2 in HER2 status, age status, PAM50 subtypes, and triple-negative breast cancer was also highly consistent with that in TCGA (all P < 0.001) (Supplementary Figure 1D–1I and Supplementary Table 1). FMO2 was dysregulated in Ki67 status, Scarff Bloom and Richardson grade status, and Nottingham Prognostic Index status (all P < 0.0001) (Supplementary Figure 1J–1L and Supplementary Table 1).

Decreased expression of FMO2 correlates with poor outcomes in breast cancer

We then analyzed the prognostic value of FMO2. There were three probe data of FMO2 (206263_at, 211726_s_at, and 228268_at) in the gene chip data of Kaplan–Meier plotter. The results indicated that a lower level of FMO2 (206263_at) significantly correlated with poor OS (HR = 0.80 (0.65~0.99), P = 0.038) (Figure 3A) and RFS (HR = 0.69 (0.62~0.77), P < 0.0001) (Figure 3B), while significantly correlated with preferable DMFS (HR = 1.44 (1.21~1.71), P < 0.0001) (Figure 3C). A lower level of FMO2 (206263_at) correlated with poor PPS with no statistical difference (HR = 0.82 (0.62~1.10), P = 0.18) (Supplementary Figure 2A). A lower level of FMO2 (211726_s_at) significantly correlated with poor OS (HR = 0.67 (0.55~0.82), P < 0.0001) (Figure 3D), PPS (HR = 0.75 (0.59~0.94), P = 0.014) (Figure 3E), and RFS (HR = 0.89 (0.80~0.99), P = 0.031) (Figure 3F), while correlated with poor DMFS with no statistical difference (HR = 0.90 (0.77~1.05), P = 0.20) (Supplementary Figure 2B). A lower level of FMO2 (228268_at) significantly correlated with poor OS (HR = 0.58 (0.44~0.76), P < 0.0001) (Figure 3G) and RFS (HR = 0.75 (0.63~0.88), P = 0.00043) (Figure 3H), while correlated with poor PPS (HR = 0.79 (0.55~1.13), P = 0.2) (Supplementary Figure 2C) and DMFS (HR = 0.82 (0.63~1.07), P = 0.14) (Supplementary Figure 2D) with no statistical difference. RNA-sequence in Kaplan–Meier plotter revealed that a lower level of FMO2 significantly correlated with worse OS (HR = 0.71 (0.56~0.90), P = 0.0039) (Figure 3I).

FMO2 correlates with N/ER/PR subgroups in breast cancer

To further investigate the role of FMO2 in breast cancer OS and DFS, we verified that FMO2 was positively correlated with OS in N+/ER all/PR+ (HR = 0.45 (0.22~0.93), P = 0.0302) (Supplementary Figure 3A), N+/ER+/PR all (HR = 0.48 (0.24~0.96), P = 0.0386) (Supplementary Figure 3B), and N+/ER+/PR+ subgroups (HR = 0.47 (0.22~0.97), P = 0.0411) (Supplementary Figure 3C) and DFS in N+/ER all/PR+ (HR = 0.46 (0.26~0.84), P = 0.0118) (Supplementary Figure 3D), N+/ER+/PR+ (HR = 0.48 (0.26~0.87), P = 0.0159) (Supplementary Figure 3E), N+/ER+/PR all (HR = 0.50 (0.29~0.88), P = 0.0169) (Supplementary Figure 3F), and N+/ER all/PR all subgroups (HR = 0.63 (0.39~1.00), P = 0.0487) (Supplementary Figure 3G) in TCGA from bc-GenExMiner. Similarly, FMO2 was positively correlated with OS in N all/ER+/PR all (HR = 0.65 (0.51~0.84), P = 0.0009) (Supplementary Figure 4A), N all/ER all/PR all (HR = 0.70 (0.57~0.87), P = 0.0015) (Supplementary Figure 4B), N all/ER+/PR+ (HR = 0.67 (0.51~0.88), P = 0.0037) (Supplementary Figure 4C), N-/ER+/PR all (HR = 0.60 (0.43~0.85), P = 0.0042) (Supplementary Figure 4D), N all/ER all/PR+ (HR = 0.70 (0.53~0.92), P = 0.0098) (Supplementary Figure 4E), N-/ER all/PR all (HR = 0.67 (0.50~0.92), P = 0.0115) (Supplementary Figure 4F), N-/ER+/PR+ (HR = 0.64 (0.44~0.92), P = 0.0171) (Supplementary Figure 4G), and N-/ER all/PR+ subgroups (HR = 0.67 (0.46~0.96), P = 0.0287) (Supplementary Figure 4H)

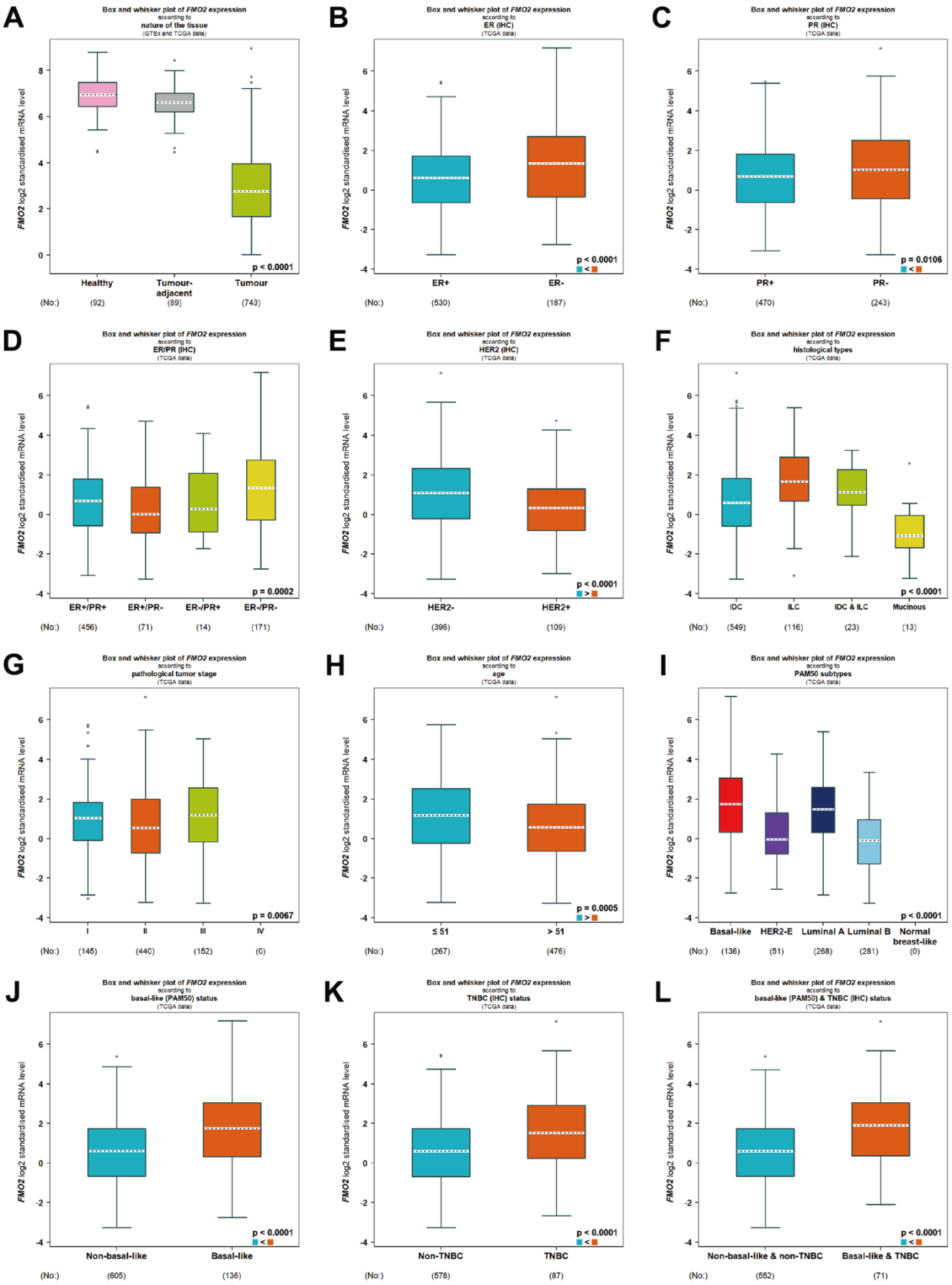

Figure 2. Relationship between FMO2 and different clinical indicators in TCGA. (**A**) Nature of the tissue. (**B**) ER status. (**C**) PR status. (**D**) ER and PR status combinations. (**E**) HER2 status. (**F**) Histological types. (**G**) Pathological tumor stage. (**H**) Age status. (**I**) PAM50 subtypes. (**J**) Basal-like (PAM50). (**K**) Triple-negative breast cancer. (**L**) Basal-like (PAM50) and triple-negative breast cancer.

and DFS in N all/ER+/PR all (HR = 0.65 (0.51~0.84), P = 0.0009) (Supplementary Figure 4I), N all/ER all/PR all (HR = 0.70 (0.57~0.87), P = 0.0015) (Supplementary Figure 4J), N all/ER+/PR+ (HR = 0.67 (0.51~0.88), P = 0.0037) (Supplementary Figure 4K), N-/ER+/PR all (HR = 0.60 (0.43~0.85), P = 0.0042) (Supplementary Figure 4L), N all/ER all/PR+ (HR = 0.70 (0.53~0.92), P = 0.0098) (Supplementary Figure 4M), N-/ER all/PR all (HR = 0.67 (0.50~0.92), P = 0.0115) (Supplementary Figure 4N), N-/ER+/PR+ (HR = 0.64 (0.44~0.92), P = 0.0171) (Supplementary Figure 4O), and N-/ER all/PR+ subgroups (HR = 0.67 (0.46~0.96), P = 0.0287) (Supplementary Figure 4P) in SCAN-B from bc-GenExMiner.

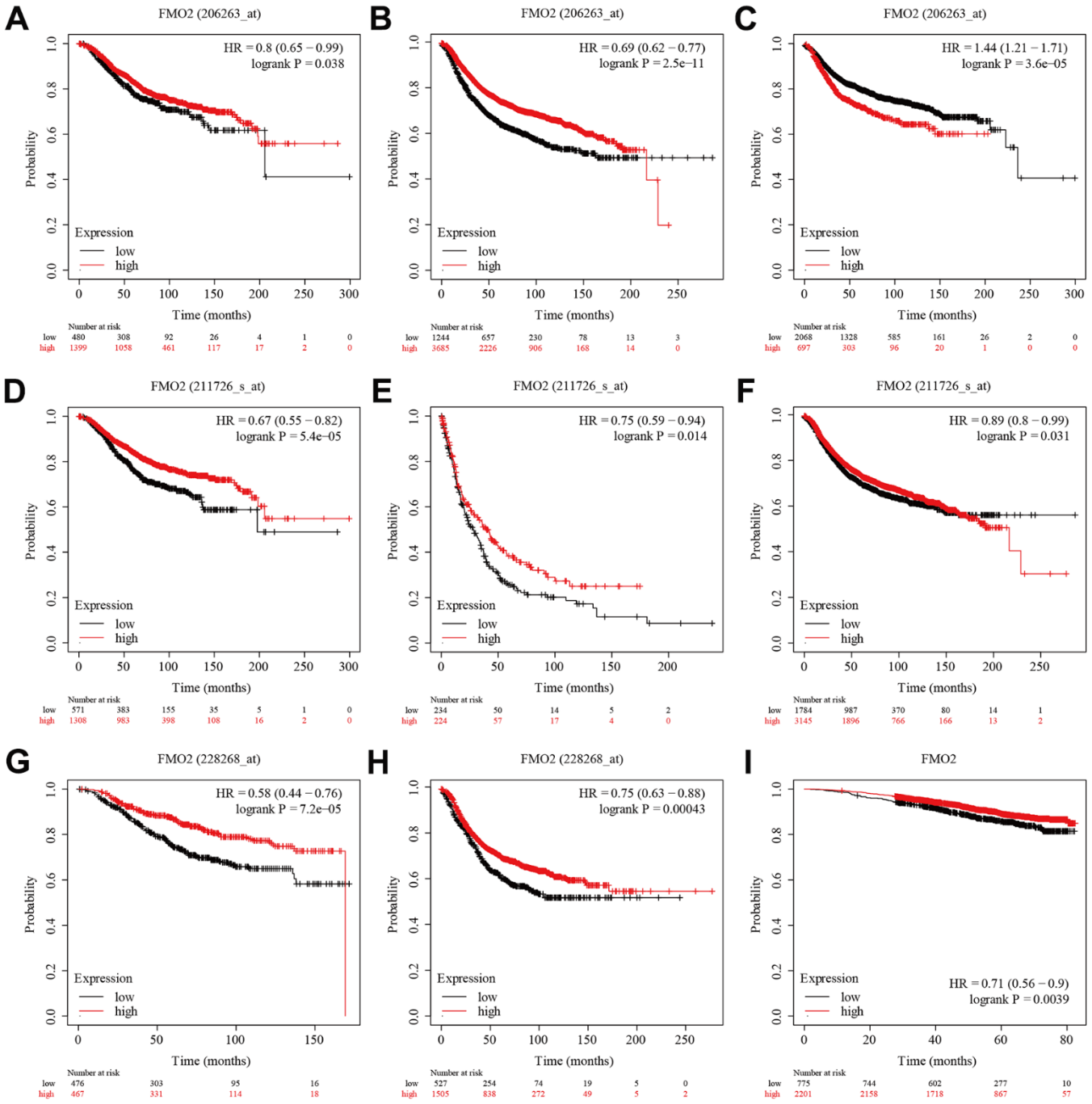

Figure 3. The survival analysis of FMO2 in the gene chip data and RNA-sequence data of Kaplan–Meier plotter. (**A**) FMO2 (206263_at) in OS. (**B**) FMO2 (206263_at) in RFS. (**C**) FMO2 (206263_at) in DMFS. (**D**) FMO2 (211726_s_at) in OS. (**E**) FMO2 (211726_s_at) in PPS. (**F**) FMO2 (211726_s_at) in PPS. (**G**) FMO2 (228268_at) in OS. (**H**) FMO2 (228268_at) in RFS. (**I**) FMO2 in OS.

Breast cancer with high FMO2 levels was sensitive to immunotherapy

Anti-programmed cell death protein 1 (PD-1), anti-programmed death-ligand 1 (PD-L1), and anti-cytotoxic T-lymphocyte antigen 4 (CTLA-4) immunotherapies are commonly used in the treatment of various cancers [28, 29]. Here, we analyzed the sensitivity of FMO2 expression to immunotherapy. Analysis of patients receiving anti-PD-1 immunotherapy suggested that patients with high FMO2 expression were more sensitive to anti-PD-1 immunotherapy in OS (HR = 0.62 (0.47~0.81), P = 0.00045) (Figure 4A). Similarly, patients with high FMO2 expression were more sensitive to anti-PD-L1 immunotherapy (HR = 0.45 (0.33~0.61), P < 0.0001) (Figure 4B) and anti-CTLA-4 immunotherapy (HR = 0.30 (0.18~0.49), P < 0.0001) in OS (Figure 4C). Subgroup analyses indicated that patients with high FMO2 expression were more sensitive to pembrolizumab immunotherapy (HR = 0.45 (0.31~0.65), P < 0.0001) (Figure 4D), nivolumab immunotherapy (HR = 0.64 (0.40~1.02), P = 0.061) (Figure 4E), atezolizumab immunotherapy (HR = 0.45 (0.33~0.62), P < 0.0001) (Figure 4F), and ipilimumab immunotherapy (HR = 0.30 (0.18~0.49), P < 0.0001) in OS (Figure 4G). The sample size of patients receiving durvalumab immunotherapy and tremelimumab immunotherapy was too small, so no analyses were conducted.

Regarding PFS, patients with high FMO2 expression were more sensitive to anti-PD-1 immunotherapy (HR = 0.49 (0.35~0.69), P < 0.0001) (Figure 5A), anti-PD-L1 immunotherapy (HR = 0.24 (0.15~0.38), P < 0.0001) (Figure 5B), and anti-CTLA-4 immunotherapy (HR = 0.28 (0.16~0.50), P < 0.0001) (Figure 5C). Subgroup analyses indicated that patients with high FMO2 expression were more sensitive to pembrolizumab immunotherapy (HR = 0.52 (0.37~0.74), P < 0.0001) (Figure 5D), nivolumab immunotherapy (HR = 0.43 (0.22~0.85), P = 0.012) (Figure 5E), atezolizumab immunotherapy (HR = 0.24 (0.14~0.40), P < 0.0001) (Figure 5F), durvalumab immunotherapy (HR = 0.38 (0.14~1.02), P =0.047) (Figure 5G), and ipilimumab immunotherapy (HR = 0.28 (0.16~0.50), P < 0.0001) in OS (Figure 5H). The sample size of patients receiving tremelimumab immunotherapy was too small, so no analysis was conducted.

SFRP1 was positively correlated with FMO2 in breast cancer

Through TNMplot, we obtained 96 positive correlation genes and 10 negative correlation genes in gene chip data and 1149 positive correlation genes and 1 negative correlation gene in RNA-sequence data, respectively. The top 10 correlation genes are shown in Supplementary Table 2. Then we identified that SFRP1

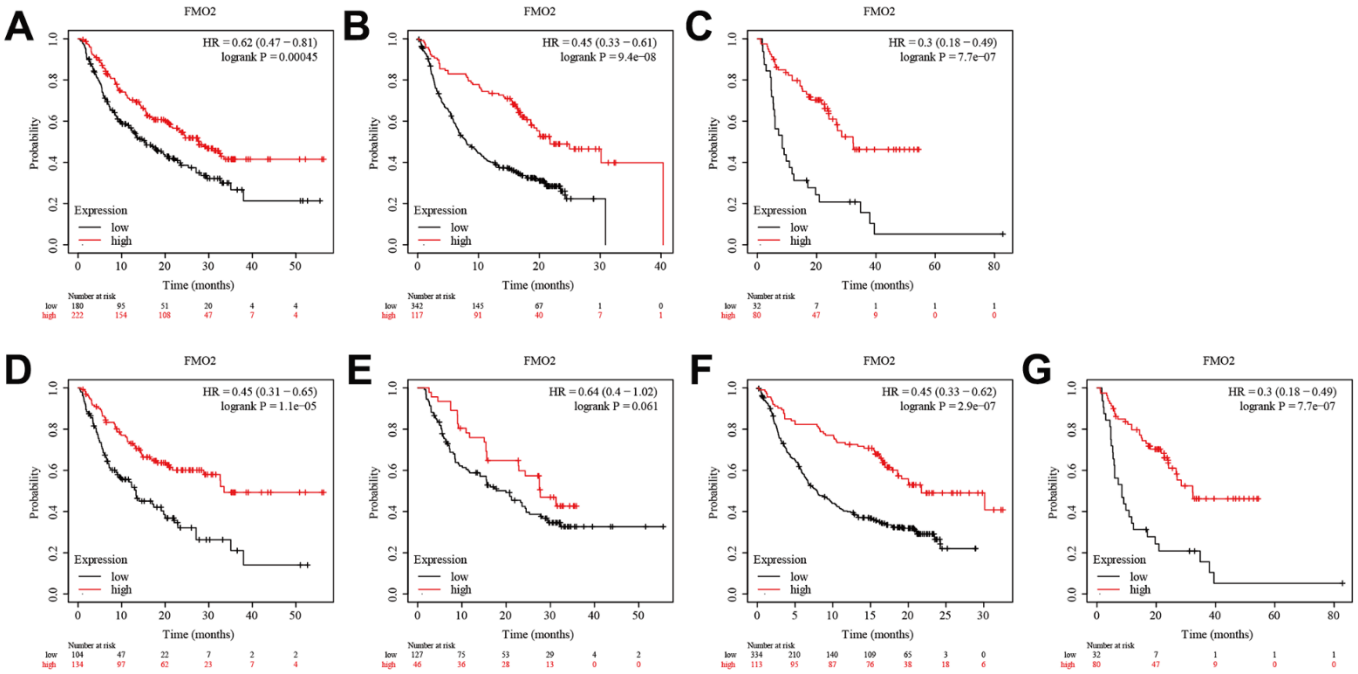

Figure 4. High FMO2 expression was sensitive to immunotherapy in OS. (**A**) Anti-PD-1 immunotherapy. (**B**) Anti-PD-L1 immunotherapy. (**C**) Anti-CTLA-4 immunotherapy. (**D**) Pembrolizumab immunotherapy. (**E**) Nivolumab immunotherapy. (**F**) Atezolizumab immunotherapy. (**G**) Ipilimumab immunotherapy.

was positively correlated with FMO2 in breast cancer through the Venn diagram (Figure 6A, 6B) and ranks (Supplementary Table 2). The scatter diagrams showed that SFRP1 was positively correlated with FMO2 in breast cancer in gene chip data (Figure 6C) and RNA-sequence data (Figure 6D). Finally, we validated the co-expression profile of FMO2 and SFRP1 in 8246 patients with breast cancer with DNA microarrays data (Figure 6E) and 4421 patients with breast cancer with RNA-sequence data (Figure 6F) from bc-GenExMiner and 1284 patients with breast cancer with TCGA breast cancer data from UCSC Xena (Figure 6G). The density plots indicated that the expression trend of FMO2 and SFRP1 in the normal, tumor, and metastatic tissues were consistent, regardless of gene chip data (Figure 6H) and RNA-sequence data (Figure 6I).

SFRP1 was downregulated in breast cancer

The pan-cancer analysis indicated SFRP1 mRNA expression is downregulated in various cancers (Supplementary Figure 5A), including breast cancer. Furthermore, both gene chip data and RNA sequencing data showed that SFRP1 mRNA expression in breast cancer was significantly reduced, and the expression in metastatic breast cancer is lower (Supplementary Figure 5B, 5C). Then TCGA database including 1097 breast invasive carcinoma patients and 114 normal patients showed SFRP1 mRNA expression was indeed downregulated ($P < 0.0001$) (Supplementary Figure 5D). The Clinical Proteomic Tumor Analysis Consortium (CPTAC) database including 125 breast cancer patients and 18 normal patients showed that SFRP1 protein expression was downregulated ($P < 0.0001$) (Supplementary Figure 5E).

We next compared SFRP1 expression in different subtypes of breast cancer according to different clinical indicators. In the TCGA database, SFRP1 was downregulated in breast cancer compared to healthy regardless of individual cancer stages (Figure 7A), race (Figure 7B), nodal metastasis status (Figure 7C), tumor histology (Figure 7D), major subclasses (Figure 7E), menopause status (Figure 7F), and TP53 mutation status (Figure 7G). Similarly, In the CPTAC database, SFRP1 was downregulated in breast cancer compared to healthy regardless of individual cancer stages (Figure 7H), race (Figure 7I), tumor histology (Figure 7J), and major subclasses (Figure 7K).

SFRP1 was hypermethylation in breast cancer

After confirming that SFRP1 was highly expressed in breast cancer, we further explored the SFRP1 promoter methylation level, and the results showed that SFRP1 was hypermethylation in breast cancer

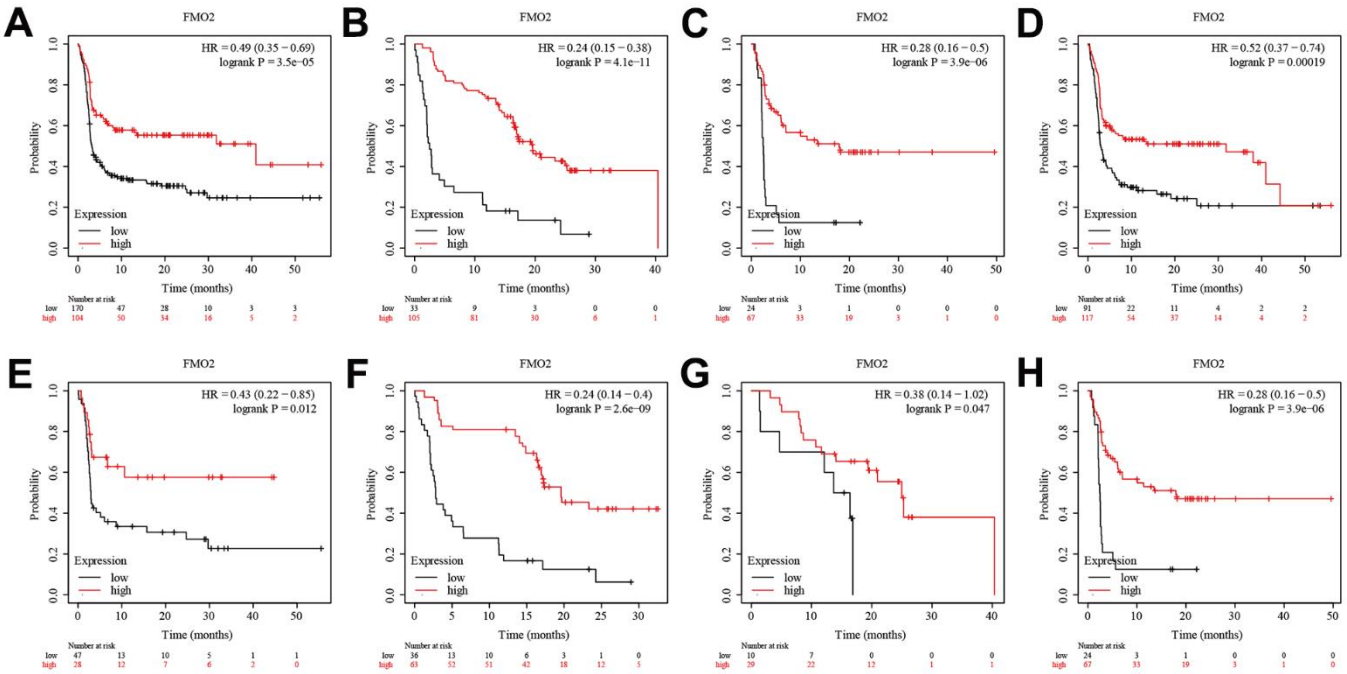

Figure 5. High FMO2 expression was sensitive to immunotherapy in PFS. (**A**) Anti-PD-1 immunotherapy. (**B**) Anti-PD-L1 immunotherapy. (**C**) Anti-CTLA-4 immunotherapy. (**D**) Pembrolizumab immunotherapy. (**E**) Nivolumab immunotherapy. (**F**) Atezolizumab immunotherapy. (**G**) Durvalumab immunotherapy. (**H**) Ipilimumab immunotherapy.

(Supplementary Figure 6A), regardless of individual cancer stages (Supplementary Figure 6B), race (Supplementary Figure 6C), nodal metastasis status (Supplementary Figure 6D), tumor histology (Supplementary Figure 6E), major subclasses (Supplementary Figure 6F), menopause status (Supplementary Figure 6G), and TP53 mutation status (Supplementary Figure 6H).

SFRP1 could act as a predictive biomarker in breast cancer

Through ROCplot, we found that SFRP1 (202037_s_at) was correlated to pathological complete response in breast cancer regardless of any chemotherapy (taxane, anthracycline, ixabepilone, CMF (cyclophosphamide, methotrexate, and fluorouracil), FAC (fluorouracil, Adriamycin, and cytoxan), or FEC (fluorouracil, epirubicin, and cyclophosphamide)) (AUC = 0.578, P < 0.0001) (Supplementary Figure 7A), hormone therapy (tamoxifen or aromatase inhibitor) (AUC = 0.629, P = 0.048) (Supplementary Figure 7B), and anti-HER2 therapy (trastuzumab or lapatinib) (AUC = 0.566, P = 0.047) (Supplementary Figure 7C). Regarding relapse-free survival status at 5 years, SFRP1 could act as a predictive biomarker to predict chemotherapy response (AUC = 0.530, P = 0.130) (Supplementary Figure 7D), hormone therapy response (tamoxifen or aromatase inhibitor) (AUC = 0.604, P < 0.0001) (Supplementary Figure 7E), and anti-HER2 therapy response (trastuzumab or lapatinib) (AUC = 0.516, P = 0.430) (Supplementary Figure 7F).

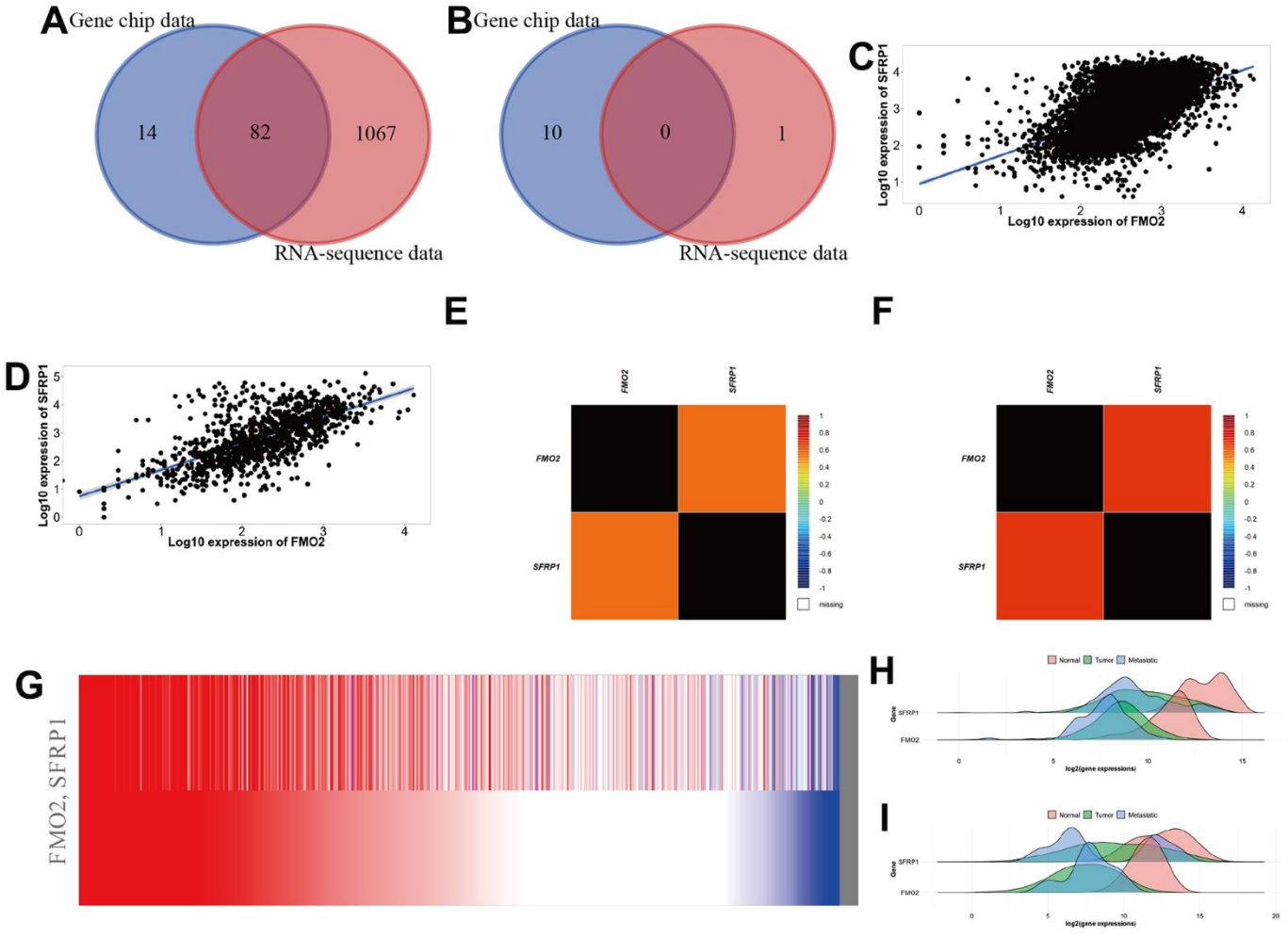

Figure 6. SFRP1 was positively correlated with FMO2 in breast cancer. (**A**) Venn diagram of positive correlation genes in TNMplot. (**B**) Venn diagram of negative correlation genes in TNMplot. (**C**) Scatter diagram in gene chip data of TNMplot. (**D**) Scatter diagram in RNA-sequence data of TNMplot. (**E**) Heat map in DNA microarrays data of bc-GenExMiner. (**F**) Heat map in RNA-sequence data of bc-GenExMiner. (**G**) Heat map in TCGA breast cancer data of UCSC Xena. (**H**) Density plot in gene chip data of TNMplot. (**I**) Density plot in RNA-sequence data of TNMplot.

SFRP1 regulated breast cancer indecently of the Wnt signal pathway

We conducted gene ontology (cellular component, molecular function, and biological process) and Kyoto Encyclopedia of Genes and Genomes pathway analyses. Enrichment results with weighted set cover redundancy reduction indicated that extracellular matrix, vesicle lumen, nuclear speck, and intrinsic component of endoplasmic reticulum membrane were enriched in cellular component (Figure 8A); extracellular matrix structural constituent, structural constituent of cytoskeleton, mRNA binding, and ribonucleoprotein complex binding were enriched in molecular function (Figure 8B); extracellular structure organization, regulation of inflammatory response, mRNA processing, and mitochondrial gene expression were enriched in biological process (Figure 8C); and

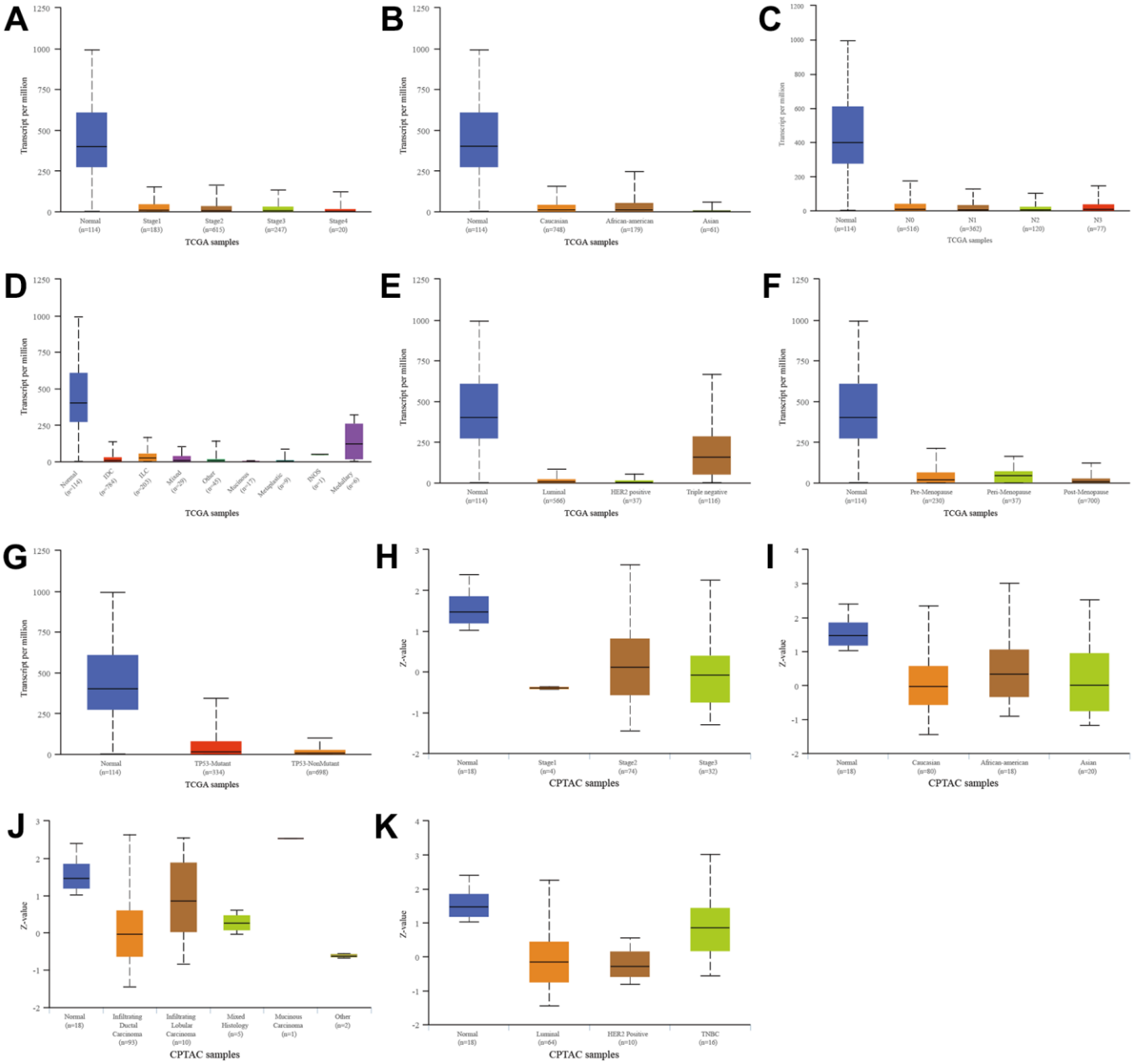

Figure 7. Relationship between SFRP1 and different clinical indicators. (**A**) Individual cancer stages in TCGA. (**B**) Race in TCGA. (**C**) Nodal metastasis status in TCGA. (**D**) Tumor histology in TCGA. (**E**) Major subclasses in TCGA. (**F**) Menopause status in TCGA. (**G**) TP53 mutation status in TCGA. (**H**) Individual cancer stages in CPTAC. (**I**) Race in CPTAC. (**J**) Tumor histology in CPTAC. (**K**) Major subclasses in CPTAC.

component and coagulation cascades, focal adhesion, protein export, and spliceosome were enriched in Kyoto Encyclopedia of Genes and Genomes pathway (Figure 8D–8G). In general, SFRP1 predicted the therapeutic response of breast cancer indecently of the Wnt signal pathway.

DISCUSSION

It is reported that breast cancer is related to abnormal expression of oncogenes [30]. Although the diagnosis, treatment, and prognosis of breast cancer have improved, it is still the most common malignant tumor with the highest incidence rate among women in the world. Identification of new biomarkers of breast cancer is crucial to its diagnosis, treatment, and prognosis. Here, we confirmed that FMO2 is downregulated in breast cancer and FMO2 expression was related to clinical indicators. We later found that decreased expression of FMO2 correlates with poor OS, RFS, PPS, and DMFS. Moreover, FMO2 correlates with N/ER/PR subgroups in OS and DFS. We also explored the reason why upregulated FMO2 expression can benefit breast cancer patients, and the results showed that the high expression of FMO2 may increase the sensitivity of patients to immunotherapy. In addition, correlation analysis showed that SFRP1 is the most potentially related (positively) gene, and more importantly, SFRP1 expression was downregulated in breast cancer patients, which was consistent with FMO2 expression. Then we found that the downregulation of SFRP1 expression may be due to its hypermethylation. SFRP1 was correlated to pathological complete response and relapse-free survival status at 5 years in breast cancer regardless of any chemotherapy, hormone therapy, and anti-HER2 therapy, therefore, SFRP1 could act as a predictive biomarker to predict response among patients with breast cancer. Finally, the functional analysis indicated

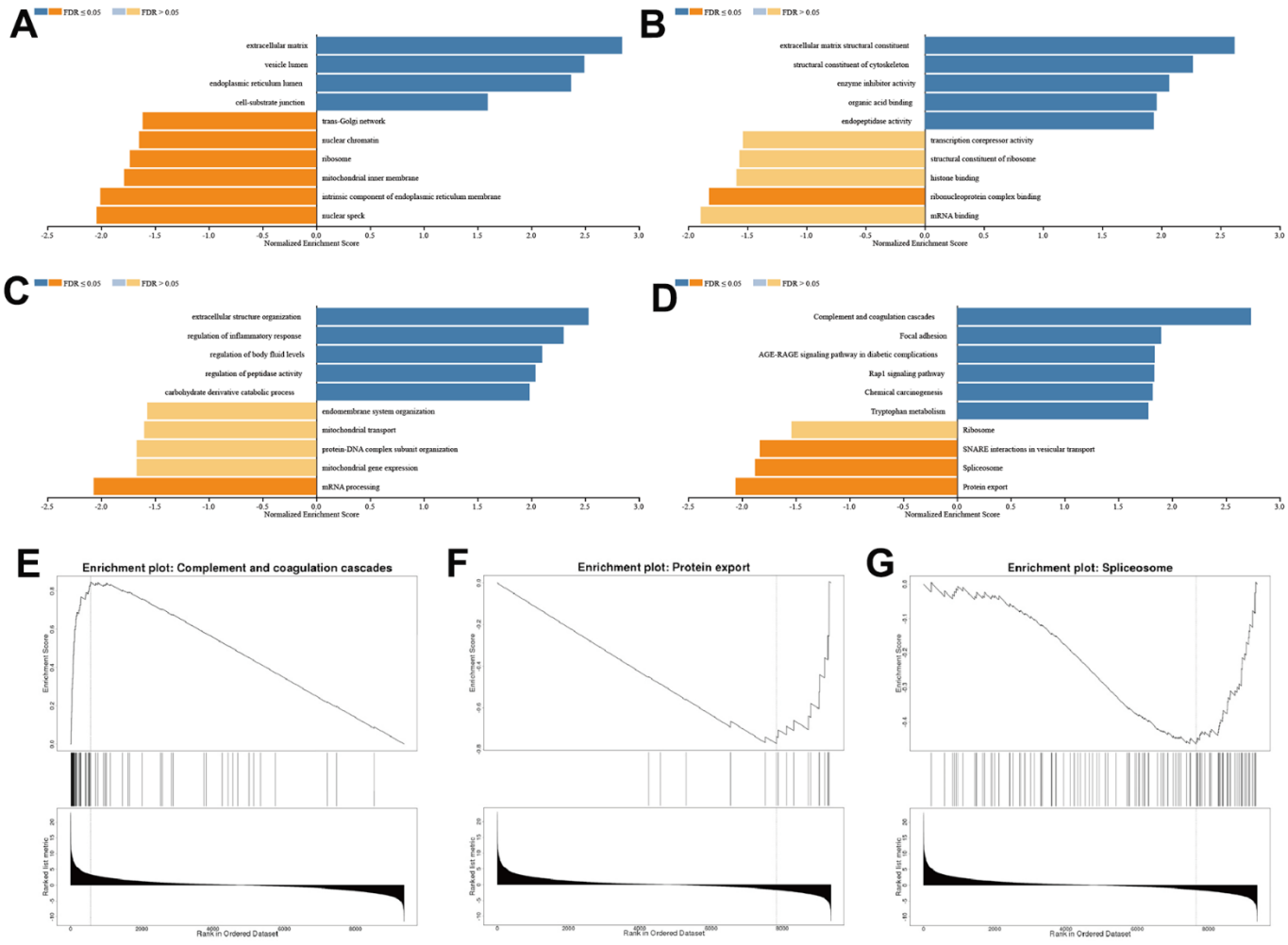

Figure 8. SFRP1 regulated extracellular matrix in breast cancer. (**A**) Cellular component. (**B**) Molecular function. (**C**) Biological process. (**D**) Kyoto Encyclopedia of Genes and Genomes pathway. (**E**) Component and coagulation cascades. (**F**) Protein export. (**G**) Spliceosome.

that SFRP1 might regulate the extracellular matrix to influence component and coagulation cascades, focal adhesion, protein export, and spliceosome pathways in breast cancer.

Up to now, there have been relatively few studies on FMO2 in breast cancer. A new high-throughput drug metabolizing enzymes and transporters microarray platform revealed that single nucleotide polymorphism in FMO2 was significantly associated with docetaxel-induced febrile neutropenia in Lebanese breast cancer patients [31]. FMO2, located within the candidate gains on 1q and is known to be overexpressed in invasive lobular carcinoma relative to invasive ductal carcinoma, which was consistent with our results, with genetic subgroups differed with regard to histology, tumor grading, frequency of alterations, and ER expression [32]. SFRP1 contains a cysteine-rich domain homologous to the putative Wnt-binding site of Frizzled proteins [33, 34]. A previous study found that FMO2 and SFRP1 were under-expressed in ductal carcinoma [35], a common type of breast cancer. Here, we for the first time found SFRP1 positively correlates with FMO2. The promoter hypermethylation is the predominant mechanism of SFRP1 gene silencing in breast cancer [36, 37], importantly, our findings demonstrate this epi-genetic mechanism again. Previous studies have shown that SFRP1 can be used as a prognostic marker in breast cancer [36–38] and SFRP1 might be used as a marker for chemotherapy and neoadjuvant chemotherapy response in triple-negative breast cancer [39, 40]. In addition to chemotherapy, we proved that SFRP1 can be used as a predictive marker of hormone therapy and anti-HER2 therapy. SFRP1 interferences with Wnt signaling to block the ligand-receptor interaction [41] or co-regulates with BDNF [42] to have a potential inhibitory effect on breast cancer. Interestingly, we found that SFRP1 affects breast cancer independently of the Wnt signal pathway.

This study has many advantages. Firstly, we proposed for the first time that FMO2 can affect the effect of immunotherapy as a prognostic marker and SFRP1 could be a predictive marker of chemotherapy, hormone therapy, and anti-HER2 therapy on breast cancer. Secondly, we found that FMO2 inhibits breast cancer through co-expression with SFRP1, and the latter plays a role through non-Wnt signal pathway, which is also not reported. Finally, all our research results are basically verified with different data, which makes our research results more robust. Our research also has many areas for improvement. Primally, we confuse all types of breast cancer to solve this huge problem. The prognosis and predictive role of FMO2 and SFRP1 for different types of breast cancer still need further research. In addition, this study is mainly based on existing data and lacks extensive experimental and clinical validation. These markers need more validation before the widespread adoption of treatment decisions for breast cancer.

In conclusion, this analysis revealed that FMO2 was lower expressed in breast cancer compared with normal tissues and contributes to subtype classification and prognosis prediction with co-expressed SFRP1, which could be considered as a predictive biomarker for breast cancer treatment indecently of the Wnt signal pathway by affecting the extracellular matrix.

AUTHOR CONTRIBUTIONS

Feng Lu conceived and designed the article. Lichun Wu and Jie Chu collected the data. Lichun Wu, Jie Chu, Lijuan Shangguan, Mingfei Cao, and Feng Lu analyzed the data. Lichun Wu, Jie Chu, and Feng Lu visualized the results. All authors interpreted the results. Lichun Wu and Jie Chu drafted the manuscript. Feng Lu revised the manuscript. All authors reviewed and approved the manuscript.

CONFLICTS OF INTEREST

The authors declare that they have no conflicts of interest.

FUNDING

This work was supported by the Chengdu Medical Research Project [grant number 2022417].

REFERENCES

1. Sung H, Ferlay J, Siegel RL, Laversanne M, Soerjomataram I, Jemal A, Bray F. Global Cancer Statistics 2020: GLOBOCAN Estimates of Incidence and Mortality Worldwide for 36 Cancers in 185 Countries. CA Cancer J Clin. 2021; 71:209–49. https://doi.org/10.3322/caac.21660 PMID:33538338

2. Herzog SK, Fuqua SAW. ESR1 mutations and therapeutic resistance in metastatic breast cancer: progress and remaining challenges. Br J Cancer. 2022; 126:174–86. https://doi.org/10.1038/s41416-021-01564-x PMID:34621045

3. Siegel RL, Miller KD, Fuchs HE, Jemal A. Cancer statistics, 2022. CA Cancer J Clin. 2022; 72:7–33. https://doi.org/10.3322/caac.21708 PMID:35020204

4. Houghton SC, Hankinson SE. Cancer Progress and Priorities: Breast Cancer. Cancer Epidemiol Biomarkers Prev. 2021; 30:822–44. https://doi.org/10.1158/1055-9965.EPI-20-1193

PMID:33947744

5. Wang XF, Liang B, Chen C, Zeng DX, Zhao YX, Su N, Ning WW, Yang W, Huang JA, Gu N, Zhu YH. Long Intergenic Non-protein Coding RNA 511 in Cancers. Front Genet. 2020; 11:667. https://doi.org/10.3389/fgene.2020.00667 PMID:32733536

6. Zhang A, Wang X, Fan C, Mao X. The Role of Ki67 in Evaluating Neoadjuvant Endocrine Therapy of Hormone Receptor-Positive Breast Cancer. Front Endocrinol (Lausanne). 2021; 12:687244. https://doi.org/10.3389/fendo.2021.687244 PMID:34803903

7. Wilkinson L, Gathani T. Understanding breast cancer as a global health concern. Br J Radiol. 2022; 95:20211033. https://doi.org/10.1259/bjr.20211033 PMID:34905391

8. Krueger SK, Yueh MF, Martin SR, Pereira CB, Williams DE. Characterization of expressed full-length and truncated FMO2 from rhesus monkey. Drug Metab Dispos. 2001; 29:693–700. PMID:11302936

9. Ni C, Chen Y, Xu Y, Zhao J, Li Q, Xiao C, Wu Y, Wang J, Wang Y, Zhong Z, Zhang L, Wu R, Liu Q, et al. Flavin Containing Monooxygenase 2 Prevents Cardiac Fibrosis via CYP2J3-SMURF2 Axis. Circ Res. 2022. [Epub ahead of print]. https://doi.org/10.1161/CIRCRESAHA.122.320538 PMID:35861735

10. Yu S, Yang R, Xu T, Li X, Wu S, Zhang J. Cancer-associated fibroblasts-derived FMO2 as a biomarker of macrophage infiltration and prognosis in epithelial ovarian cancer. Gynecol Oncol. 2022; 167:342–53. https://doi.org/10.1016/j.ygyno.2022.09.003 PMID:36114029

11. Fialka F, Gruber RM, Hitt R, Opitz L, Brunner E, Schliephake H, Kramer FJ. CPA6, FMO2, LGI1, SIAT1 and TNC are differentially expressed in early- and late-stage oral squamous cell carcinoma--a pilot study. Oral Oncol. 2008; 44:941–8. https://doi.org/10.1016/j.oraloncology.2007.10.011 PMID:18234543

12. Ren L, Chen H, Song J, Chen X, Lin C, Zhang X, Hou N, Pan J, Zhou Z, Wang L, Huang D, Yang J, Liang Y, et al. MiR-454-3p-Mediated Wnt/β-catenin Signaling Antagonists Suppression Promotes Breast Cancer Metastasis. Theranostics. 2019; 9:449–65. https://doi.org/10.7150/thno.29055 PMID:30809286

13. Bartha Á, Győrffy B. TNMplot.com: A Web Tool for the Comparison of Gene Expression in Normal, Tumor and Metastatic Tissues. Int J Mol Sci. 2021; 22:2622. https://doi.org/10.3390/ijms22052622 PMID:33807717

14. Chandrashekar DS, Karthikeyan SK, Korla PK, Patel H, Shovon AR, Athar M, Netto GJ, Qin ZS, Kumar S, Manne U, Creighton CJ, Varambally S. UALCAN: An update to the integrated cancer data analysis platform. Neoplasia. 2022; 25:18–27. https://doi.org/10.1016/j.neo.2022.01.001 PMID:35078134

15. Saal LH, Vallon-Christersson J, Häkkinen J, Hegardt C, Grabau D, Winter C, Brueffer C, Tang MH, Reuterswärd C, Schulz R, Karlsson A, Ehinger A, Malina J, et al. The Sweden Cancerome Analysis Network - Breast (SCAN-B) Initiative: a large-scale multicenter infrastructure towards implementation of breast cancer genomic analyses in the clinical routine. Genome Med. 2015; 7:20. https://doi.org/10.1186/s13073-015-0131-9 PMID:25722745

16. Brueffer C, Vallon-Christersson J, Grabau D, Ehinger A, Häkkinen J, Hegardt C, Malina J, Chen Y, Bendahl PO, Manjer J, Malmberg M, Larsson C, Loman N, et al. Clinical Value of RNA Sequencing-Based Classifiers for Prediction of the Five Conventional Breast Cancer Biomarkers: A Report From the Population-Based Multicenter Sweden Cancerome Analysis Network-Breast Initiative. JCO Precis Oncol. 2018; 2:PO.17.00135. https://doi.org/10.1200/PO.17.00135 PMID:32913985

17. Jézéquel P, Gouraud W, Ben Azzouz F, Guérin-Charbonnel C, Juin PP, Lasla H, Campone M. bc-GenExMiner 4.5: new mining module computes breast cancer differential gene expression analyses. Database (Oxford). 2021; 2021:baab007. https://doi.org/10.1093/database/baab007 PMID:33599248

18. Lánczky A, Győrffy B. Web-Based Survival Analysis Tool Tailored for Medical Research (KMplot): Development and Implementation. J Med Internet Res. 2021; 23:e27633. https://doi.org/10.2196/27633 PMID:34309564

19. Győrffy B. Survival analysis across the entire transcriptome identifies biomarkers with the highest prognostic power in breast cancer. Comput Struct Biotechnol J. 2021; 19:4101–9. https://doi.org/10.1016/j.csbj.2021.07.014 PMID:34527184

20. Ősz Á, Lánczky A, Győrffy B. Survival analysis in breast cancer using proteomic data from four independent datasets. Sci Rep. 2021; 11:16787. https://doi.org/10.1038/s41598-021-96340-5

PMID:34408238

21. Kovács SA, Győrffy B. Transcriptomic datasets of cancer patients treated with immune-checkpoint inhibitors: a systematic review. J Transl Med. 2022; 20:249. https://doi.org/10.1186/s12967-022-03409-4 PMID:35641998

22. Liang B, Zhang XX, Gu N. Virtual screening and network pharmacology-based synergistic mechanism identification of multiple components contained in Guanxin V against coronary artery disease. BMC Complement Med Ther. 2020; 20:345. https://doi.org/10.1186/s12906-020-03133-w PMID:33187508

23. Liang B, Li R, Liang Y, Gu N. Guanxin V Acts as an Antioxidant in Ventricular Remodeling. Front Cardiovasc Med. 2022; 8:778005. https://doi.org/10.3389/fcvm.2021.778005 PMID:35059446

24. Liang B, Liang Y, Li R, Zhang H, Gu N. Integrating systematic pharmacology-based strategy and experimental validation to explore the synergistic pharmacological mechanisms of Guanxin V in treating ventricular remodeling. Bioorg Chem. 2021; 115:105187. https://doi.org/10.1016/j.bioorg.2021.105187 PMID:34303037

25. Goldman MJ, Craft B, Hastie M, Repečka K, McDade F, Kamath A, Banerjee A, Luo Y, Rogers D, Brooks AN, Zhu J, Haussler D. Visualizing and interpreting cancer genomics data via the Xena platform. Nat Biotechnol. 2020; 38:675–8. https://doi.org/10.1038/s41587-020-0546-8 PMID:32444850

26. Fekete JT, Győrffy B. ROCplot.org: Validating predictive biomarkers of chemotherapy/hormonal therapy/anti-HER2 therapy using transcriptomic data of 3,104 breast cancer patients. Int J Cancer. 2019; 145:3140–51. https://doi.org/10.1002/ijc.32369 PMID:31020993

27. Vasaikar SV, Straub P, Wang J, Zhang B. LinkedOmics: analyzing multi-omics data within and across 32 cancer types. Nucleic Acids Res. 2018; 46:D956–63. https://doi.org/10.1093/nar/gkx1090 PMID:29136207

28. Zhang M, Chen H, Liang B, Wang X, Gu N, Xue F, Yue Q, Zhang Q, Hong J. Prognostic Value of mRNAsi/Corrected mRNAsi Calculated by the One-Class Logistic Regression Machine-Learning Algorithm in Glioblastoma Within Multiple Datasets. Front Mol Biosci. 2021; 8:777921. https://doi.org/10.3389/fmolb.2021.777921 PMID:34938774

29. Zhou JG, Liang B, Liu JG, Jin SH, He SS, Frey B, Gu N, Fietkau R, Hecht M, Ma H, Gaipl US. Identification of 15 lncRNAs Signature for Predicting Survival Benefit of Advanced Melanoma Patients Treated with Anti-PD-1 Monotherapy. Cells. 2021; 10:977. https://doi.org/10.3390/cells10050977 PMID:33922038

30. Zu C, Zhang M, Xue H, Cai X, Zhao L, He A, Qin G, Yang C, Zheng X. Emodin induces apoptosis of human breast cancer cells by modulating the expression of apoptosis-related genes. Oncol Lett. 2015; 10:2919–24. https://doi.org/10.3892/ol.2015.3646 PMID:26722264

31. Awada Z, Haider S, Tfayli A, Bazarbachi A, El-Saghir NS, Salem Z, Shamseddine A, Taher A, Zgheib NK. Pharmacogenomics variation in drug metabolizing enzymes and transporters in relation to docetaxel toxicity in Lebanese breast cancer patients: paving the way for OMICs in low and middle income countries. OMICS. 2013; 17:353–67. https://doi.org/10.1089/omi.2013.0019 PMID:23758476

32. Stange DE, Radlwimmer B, Schubert F, Traub F, Pich A, Toedt G, Mendrzyk F, Lehmann U, Eils R, Kreipe H, Lichter P. High-resolution genomic profiling reveals association of chromosomal aberrations on 1q and 16p with histologic and genetic subgroups of invasive breast cancer. Clin Cancer Res. 2006; 12:345–52. https://doi.org/10.1158/1078-0432.CCR-05-1633 PMID:16428471

33. Chong JM, Uren A, Rubin JS, Speicher DW. Disulfide bond assignments of secreted Frizzled-related protein-1 provide insights about Frizzled homology and netrin modules. J Biol Chem. 2002; 277:5134–44. https://doi.org/10.1074/jbc.M108533200 PMID:11741940

34. Uren A, Reichsman F, Anest V, Taylor WG, Muraiso K, Bottaro DP, Cumberledge S, Rubin JS. Secreted frizzled-related protein-1 binds directly to Wingless and is a biphasic modulator of Wnt signaling. J Biol Chem. 2000; 275:4374–82. https://doi.org/10.1074/jbc.275.6.4374 PMID:10660608

35. Sultan G, Zubair S, Tayubi IA, Dahms HU, Madar IH. Towards the early detection of ductal carcinoma (a common type of breast cancer) using biomarkers linked to the PPAR(γ) signaling pathway. Bioinformation. 2019; 15:799–805. https://doi.org/10.6026/97320630015799 PMID:31902979

36. Veeck J, Niederacher D, An H, Klopocki E, Wiesmann F, Betz B, Galm O, Camara O, Dürst M, Kristiansen G, Huszka C, Knüchel R, Dahl E. Aberrant methylation of the Wnt antagonist SFRP1 in breast cancer is

associated with unfavourable prognosis. Oncogene. 2006; 25:3479–88.
https://doi.org/10.1038/sj.onc.1209386
PMID:16449975

37. Lo PK, Mehrotra J, D'Costa A, Fackler MJ, Garrett-Mayer E, Argani P, Sukumar S. Epigenetic suppression of secreted frizzled related protein 1 (SFRP1) expression in human breast cancer. Cancer Biol Ther. 2006; 5:281–6.
https://doi.org/10.4161/cbt.5.3.2384 PMID:16410723

38. Klopocki E, Kristiansen G, Wild PJ, Klaman I, Castanos-Velez E, Singer G, Stöhr R, Simon R, Sauter G, Leibiger H, Essers L, Weber B, Hermann K, et al. Loss of SFRP1 is associated with breast cancer progression and poor prognosis in early stage tumors. Int J Oncol. 2004; 25:641–9.
https://doi.org/10.3892/ijo.25.3.641 PMID:15289865

39. Schäfer SA, Hülsewig C, Barth P, von Wahlde MK, Tio J, Kolberg HC, Bernemann C, Blohmer JU, Kiesel L, Kolberg-Liedtke C. Correlation between SFRP1 expression and clinicopathological parameters in patients with triple-negative breast cancer. Future Oncol. 2019; 15:1921–38.
https://doi.org/10.2217/fon-2018-0564
PMID:31140870

40. Bernemann C, Hülsewig C, Ruckert C, Schäfer S, Blümel L, Hempel G, Götte M, Greve B, Barth PJ, Kiesel L, Liedtke C. Influence of secreted frizzled receptor protein 1 (SFRP1) on neoadjuvant chemotherapy in triple negative breast cancer does not rely on WNT signaling. Mol Cancer. 2014; 13:174.
https://doi.org/10.1186/1476-4598-13-174
PMID:25033833

41. Matsuda Y, Schlange T, Oakeley EJ, Boulay A, Hynes NE. WNT signaling enhances breast cancer cell motility and blockade of the WNT pathway by sFRP1 suppresses MDA-MB-231 xenograft growth. Breast Cancer Res. 2009; 11:R32.
https://doi.org/10.1186/bcr2317
PMID:19473496

42. Huth L, Rose M, Kloubert V, Winkens W, Schlensog M, Hartmann A, Knüchel R, Dahl E. BDNF is associated with SFRP1 expression in luminal and basal-like breast cancer cell lines and primary breast cancer tissues: a novel role in tumor suppression? PLoS One. 2014; 9:e102558.
https://doi.org/10.1371/journal.pone.0102558
PMID:25036590

SUPPLEMENTARY MATERIALS

Supplementary Figures

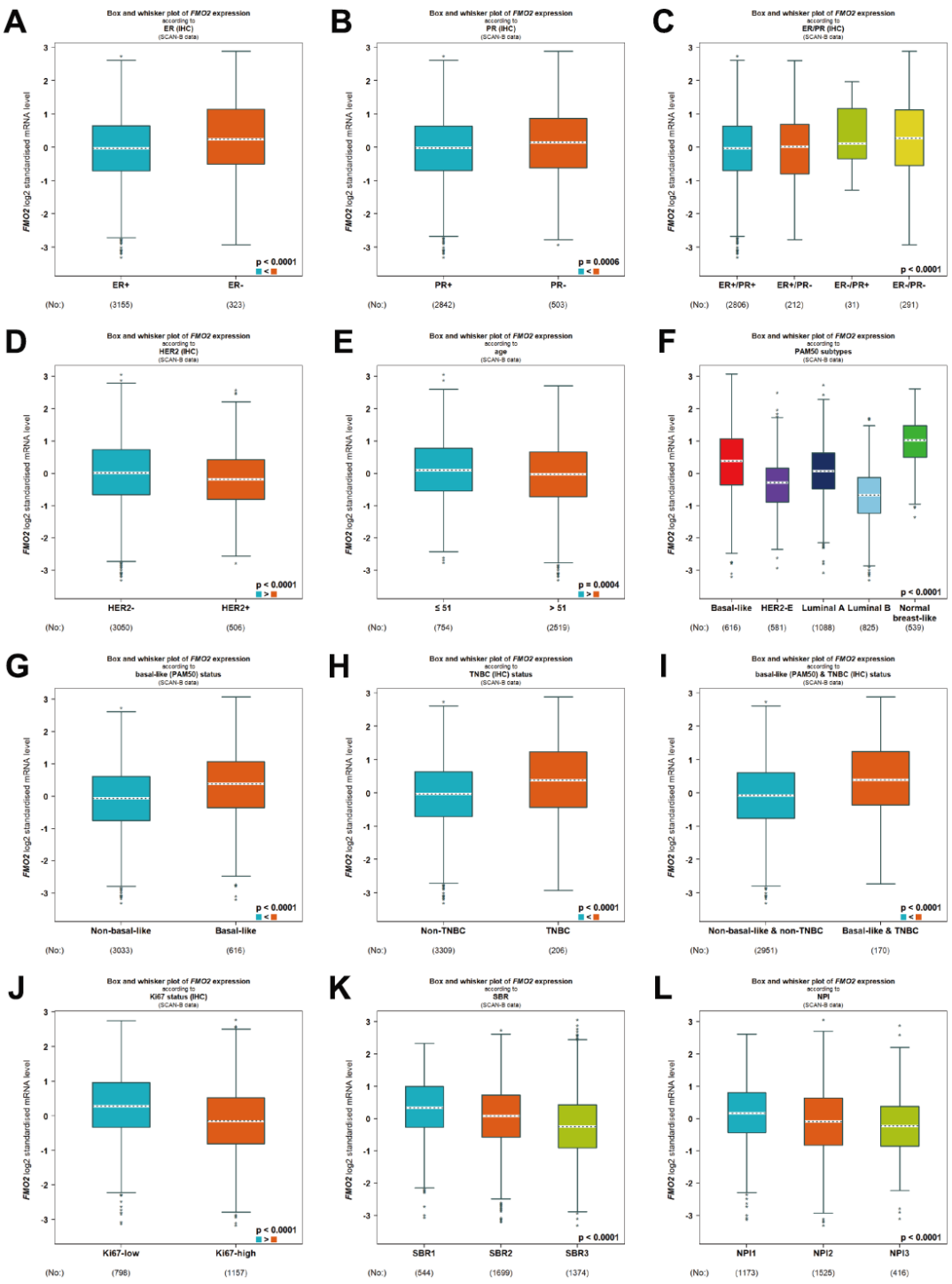

Supplementary Figure 1. Relationship between FMO2 and different clinical indicators in SCAN-B. (**A**) ER status. (**B**) PR status. (**C**) ER and PR status combinations. (**D**) HER2 status. (**E**) Age status. (**F**) PAM50 subtypes. (**G**) Basal-like (PAM50). (**H**) Triple-negative breast cancer. (**I**) Basal-like (PAM50) and triple-negative breast cancer. (**J**) Ki67 status. (**K**) Scarff Bloom and Richardson grade status. (**L**) Nottingham Prognostic Index status.

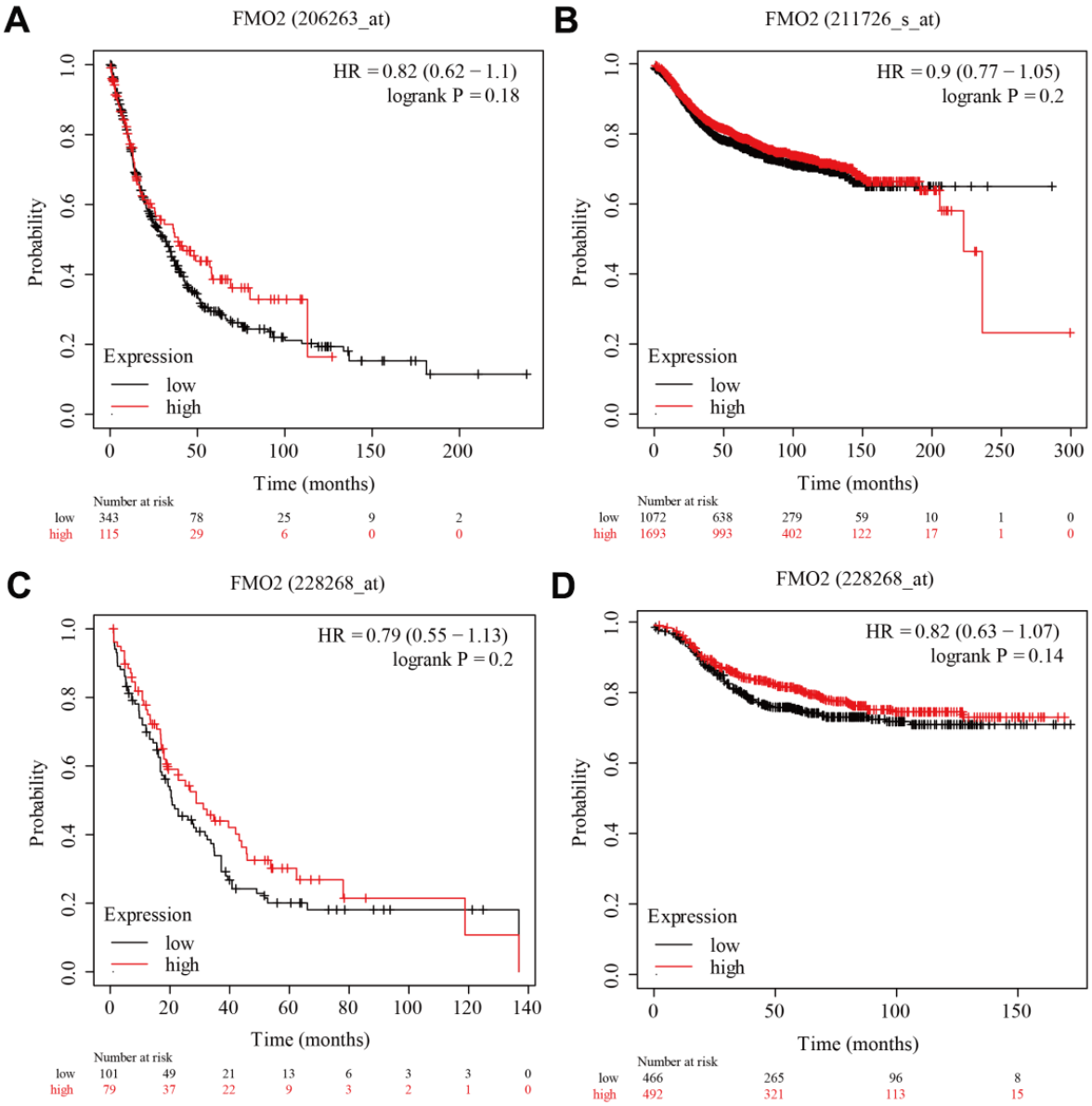

Supplementary Figure 2. The survival analysis of FMO2 in the gene chip data of Kaplan–Meier plotter. (**A**) FMO2 (206263_at) in PPS. (**B**) FMO2 (211726_s_at) in DMFS. (**C**) FMO2 (228268_at) in PPS. (**D**) FMO2 (228268_at) in DMFS.

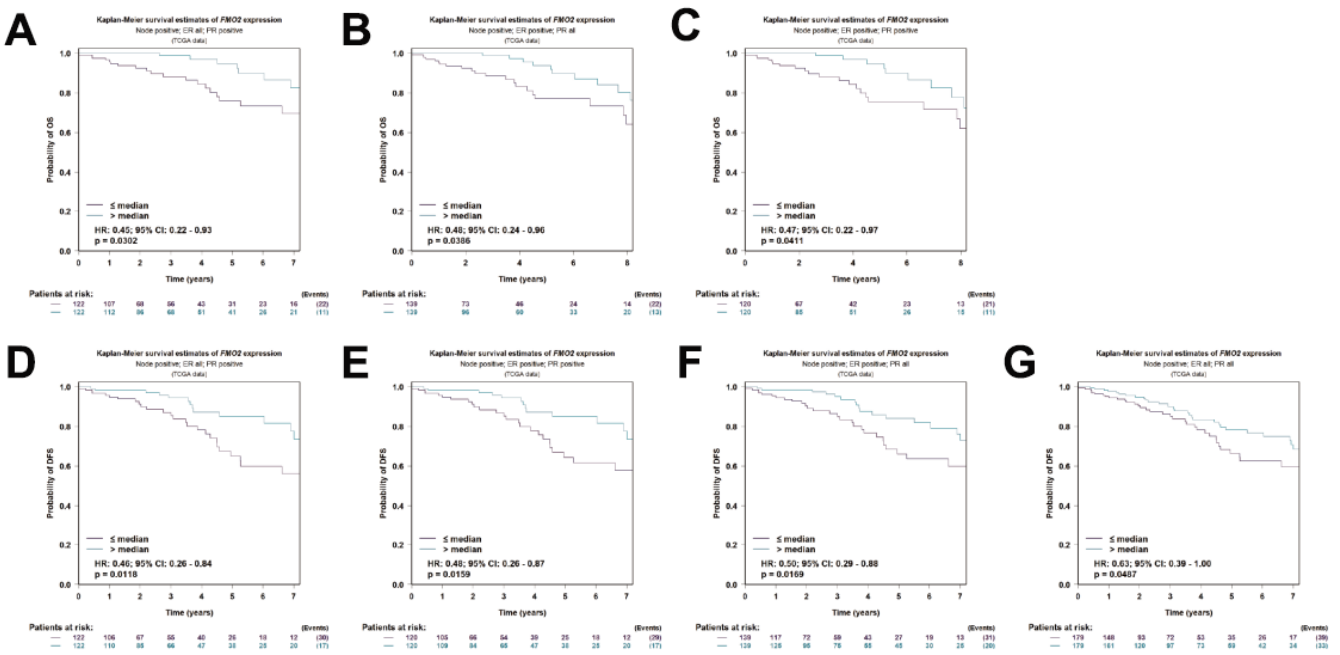

Supplementary Figure 3. The survival analysis of FMO2 in TCGA of bc-GenExMiner. (**A**) OS analysis of N+/ER all/PR+ subgroup. (**B**) OS analysis of N+/ER+/PR all subgroup. (**C**) OS analysis of N+/ER+/PR+ subgroup. (**D**) DFS analysis of N+/ER all/PR+ subgroup. (**E**) DFS analysis of N+/ER+/PR+ analysis. (**F**) DFS analysis of N+/ER+/PR all analysis. (**G**) DFS analysis of N+/ER all/PR analysis.

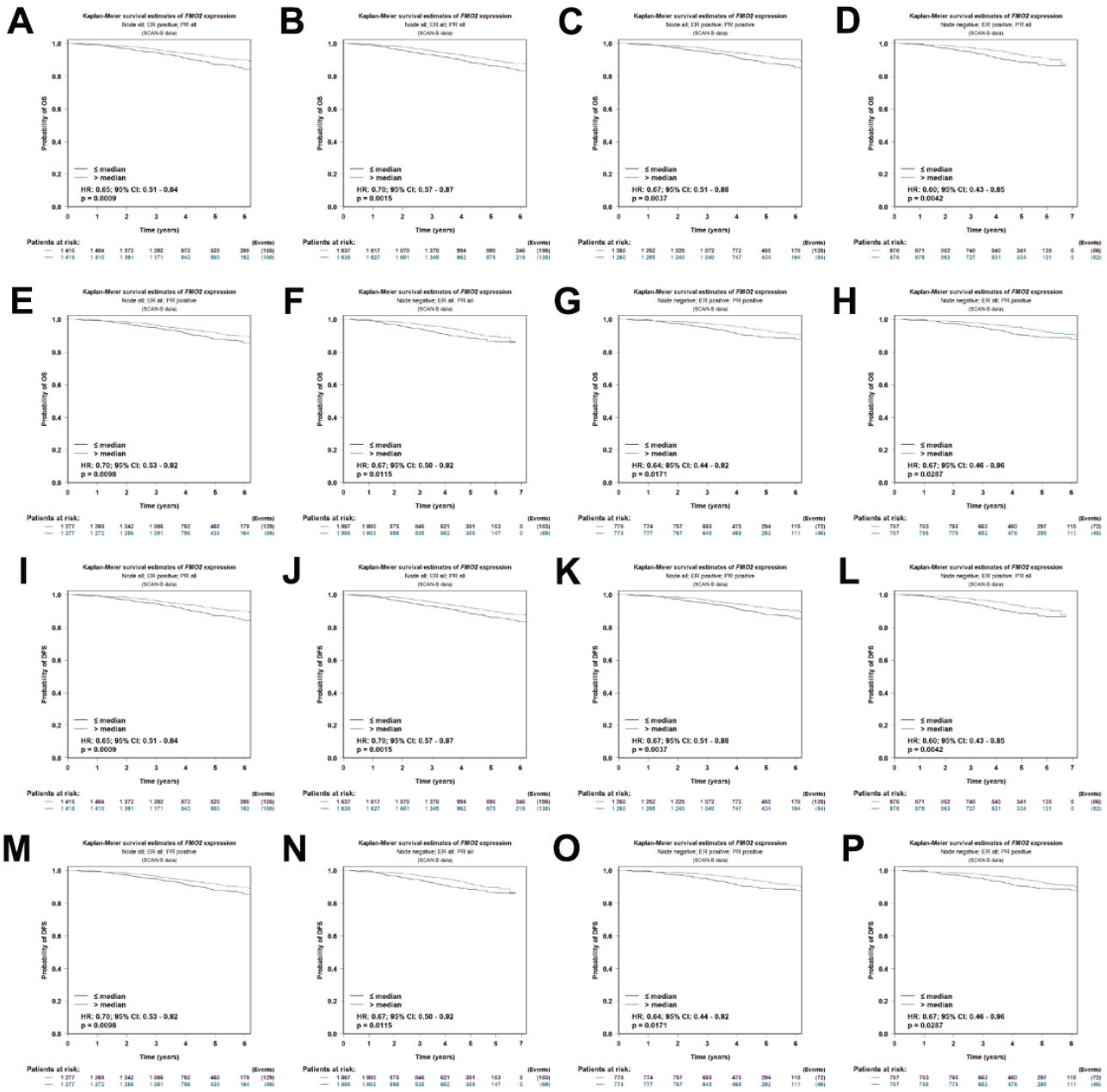

Supplementary Figure 4. The survival analysis of FMO2 in SCAN-B of bc-GenExMiner. (**A**) OS analysis of N all/ER+/PR all subgroup. (**B**) OS analysis of N all/ER all/PR all subgroup. (**C**) OS analysis of N all/ER+/PR+ subgroup. (**D**) OS analysis of N-/ER+/PR all subgroup. (**E**) OS analysis of N all/ER all/PR+ subgroup. (**F**) OS analysis of N-/ER all/PR all subgroup. (**G**) OS analysis of N-/ER+/PR+ subgroup. (**H**) OS analysis of N-/ER all/PR+ subgroup. (**I**) DFS analysis of N all/ER+/PR all subgroup. (**J**) DFS analysis of N all/ER all/PR all subgroup. (**K**) DFS analysis of N all/ER+/PR+ subgroup. (**L**) DFS analysis of N-/ER+/PR all subgroup. (**M**) DFS analysis of all/ER all/PR+ subgroup. (**N**) DFS analysis of N-/ER all/PR all subgroup. (**O**) DFS analysis of N-/ER+/PR+ subgroup. (**P**) DFS analysis of N-/ER all/PR+ subgroup.

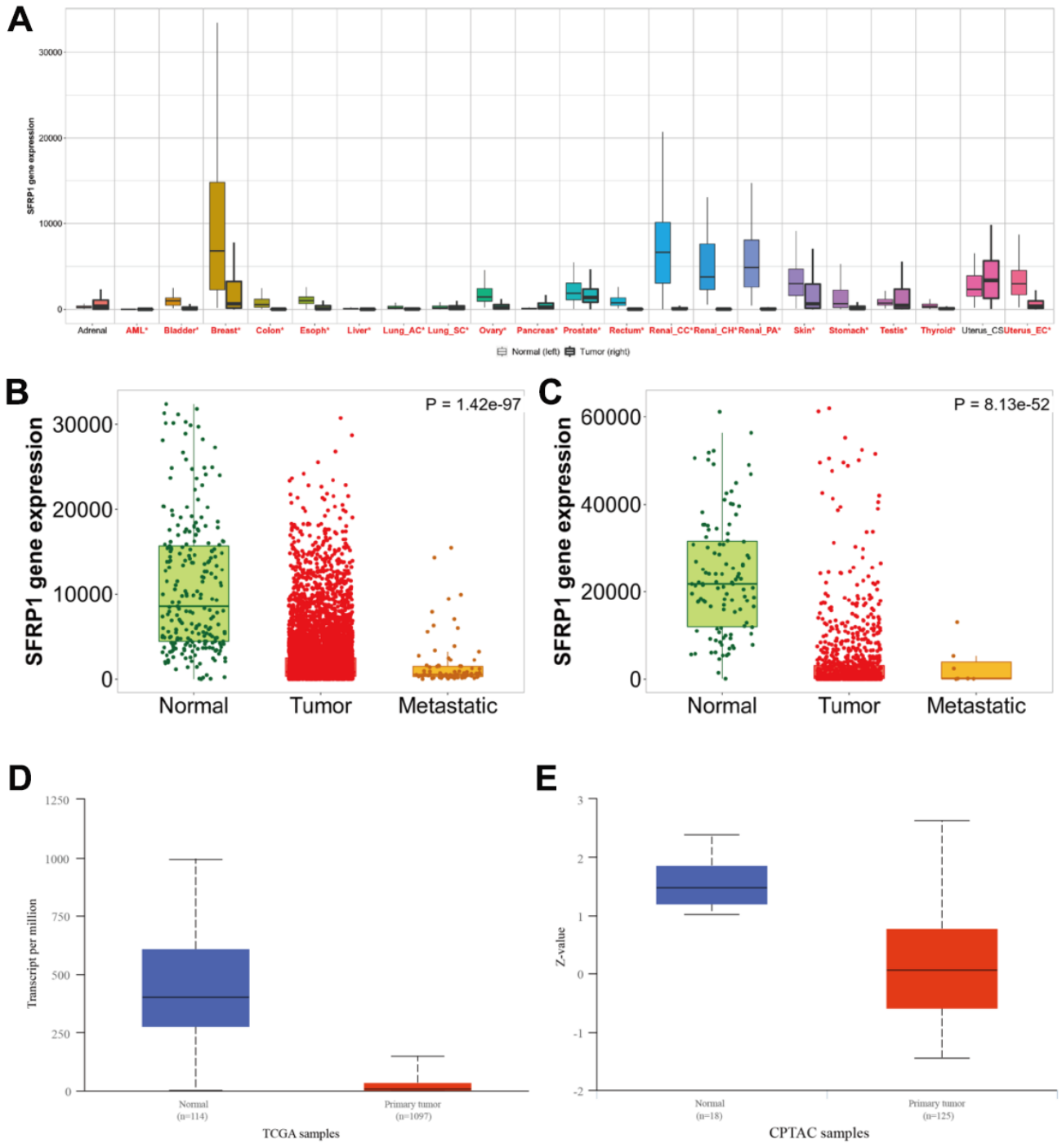

Supplementary Figure 5. The expression of SFRP1. (**A**) SFRP1 mRNA expression in pan-cancer through TNMplot. (**B**) SFRP1 mRNA expression in different breast tissues from gene chip data through TNMplot. (**C**) SFRP1 mRNA expression in different breast tissues from RNA sequences data through TNMplot. (**D**) SFRP1 mRNA expression in breast cancer through UALCAN. (**E**) SFRP1 protein expression in breast cancer through UALCAN.

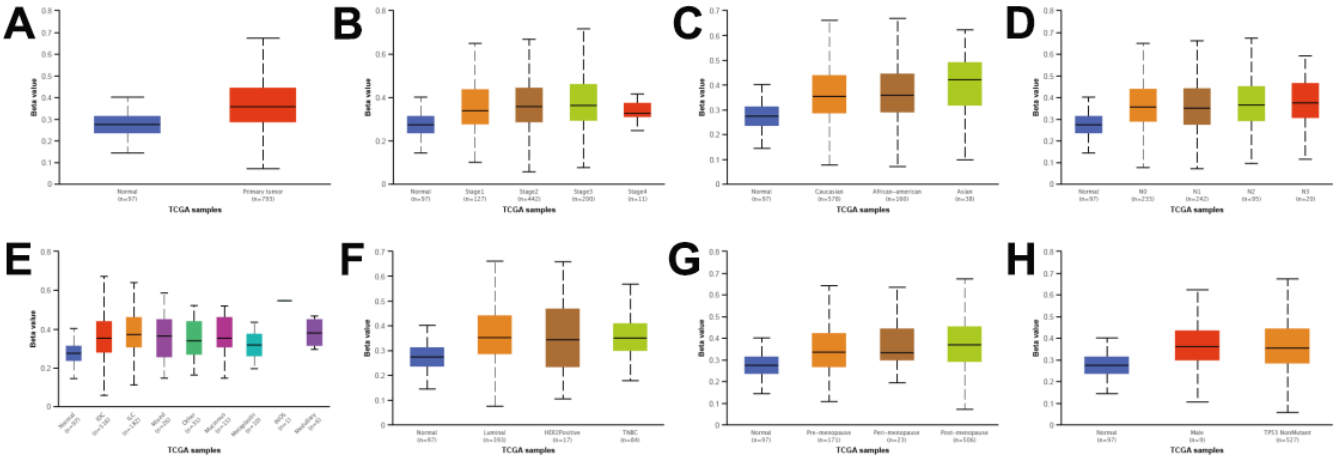

Supplementary Figure 6. SFRP1 was hypermethylation in breast cancer. (**A**) Sample types. (**B**) Individual cancer stages. (**C**) Race. (**D**) Nodal metastasis status. (**E**) Tumor histology. (**F**) Major subclasses. (**G**) Menopause status. (**H**) TP53 mutation status.

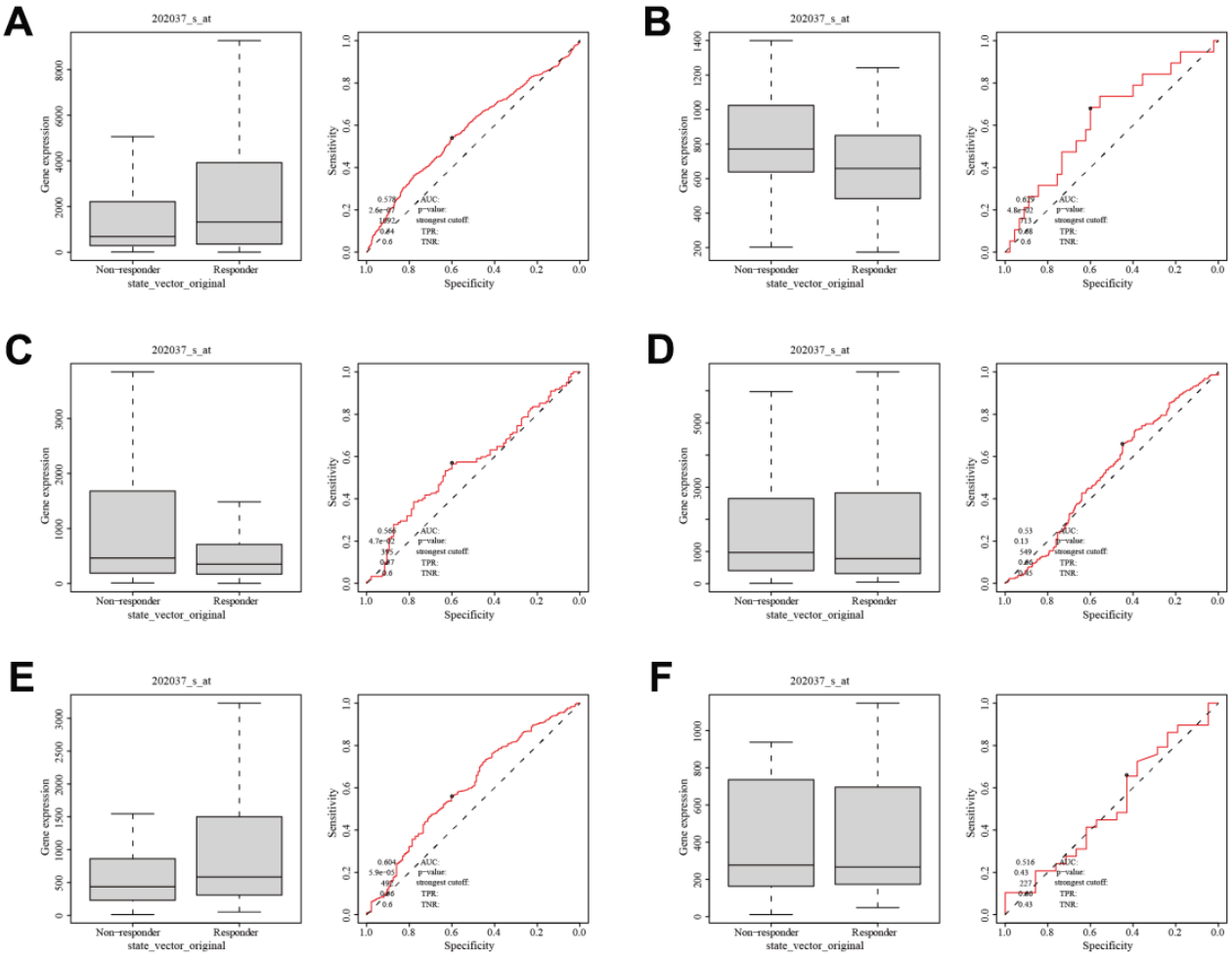

Supplementary Figure 7. SFRP1 could act as a predictive biomarker to predict therapy response. (**A**) Chemotherapy in pathological complete response. (**B**) Hormone therapy in pathological complete response. (**C**) Anti-HER2 therapy in pathological complete response. (**D**) Chemotherapy in relapse-free survival status at 5 years. (**E**) Hormone therapy in relapse-free survival status at 5 years. (**F**) Anti-HER2 therapy in relapse-free survival status at 5 years.

Supplementary Tables

Supplementary Table 1. Relationship between FMO2 and clinical parameters of breast cancer.

Variables	TCGA			SCAN-B		
	Patient number	FMO2 log2 standardized expression	P	Patient number	FMO2 log2 standardized expression	P
Nature of the tissue			< 0.0001			
Healthy	92	6.8560/ 0.7884				
Tumor-adjacent	89	6.5792/ 0.7530				
Tumor	743	2.8594/ 1.5755				
ER status			< 0.0001			< 0.0001
ER+	530	0.6034/1.7245		3155	-0.0411/0.9834	
ER-	187	1.3099/1.9443		323	0.2857/1.0738	
PR status			0.0106			0.0006
PR+	470	0.6576/1.7180		2842	-0.0337/0.9786	
PR-	243	1.0391/1.9598		503	0.1435/1.0771	
ER and PR status combinations			0.0002			< 0.0001
ER+/PR+	456	0.6589/1.7154		2806	-0.0382/0.9787	
ER+/PR-	71	0.2465/1.7630		212	-0.0454/1.0285	
ER-/PR+	14	0.6162/1.8678		31	0.2993/0.9009	
ER-/PR-	171	1.3649/1.9536		291	0.2812/1.0924	
HER2 status			< 0.0001			< 0.0001
HER2-	396	1.0139/1.7922		3050	0.0203/1.0122	
HER2+	109	0.2601/1.6170		506	-0.1702/0.9061	
Histological types			< 0.0001			
IDC	549	0.6718/1.7653				
ILC	116	1.6604/1.5374				
IDC & ILC	23	1.0332/1.7440				
Mucinous	13	0.8664/1.5635				
Pathological tumor stage			0.0067			
I	145	0.9529/1.7012				
II	440	0.6213/1.8253				
III	152	2.5408/1.8054				
Age status			0.0005			0.0004
≤ 51 years old	267	1.0975/1.8517		754	0.1071/0.9819	
> 51 years old	476	0.6083/1.7544		2519	-0.0390/1.0031	
PAM50 subtypes			< 0.0001			< 0.0001
Basal-like	136	1.6678/1.9598		616	0.3294/1.0238	
HER2-E	51	0.2343/1.5514		581	-0.3446/0.7821	
Luminal A	268	1.3893/1.5733		1088	0.0291/0.8487	
Luminal B	281	-0.1737/1.4615		825	-0.6875/0.8235	
Normal breast-like	0			539	0.9795/0.7175	
Basal-like (PAM50)			< 0.0001			< 0.0001
Non-basal-like	605	0.5807/1.7072		3033	-0.0685/0.9841	
Basal-like	136	1.6678/1.9598		616	0.3294/1.0238	
Triple-negative breast cancer			< 0.0001			< 0.0001
Non-TNBC	578	0.5983/1.7324		3309	-0.0392/0.9805	
TNBC	87	1.6091/1.9075		206	0.3626/1.1298	
TNBC & Basal-like (PAM50)			< 0.0001			< 0.0001
Non-basal-like & non-TNBC	552	0.5724/1.7088		2951	-0.0759/0.9824	
Basal-like & TNBC	71	1.7482/1.9278		170	0.3937/1.1218	
Ki67 status						< 0.0001
Ki67-low				798	0.2500/0.9643	
Ki67-high				1157	-0.1350/1.0077	

Scarff Bloom & Richardson grade status			< 0.0001
SBR1	544	0.3039/0.9245	
SBR2	1699	0.0600/0.9757	
SBR3	1374	-0.2030/1.0229	
Nottingham Prognostic Index status			< 0.0001
NPI1	1173	0.1569/0.9412	
NPI2	1525	-0.0777/1.0473	
NPI3	416	-0.2154/0.9407	

Supplementary Table 2. The top 10 correlation genes with FMO2 in breast cancer.

Gene chip data							
Positive correlations with FMO2				**Negative correlations with FMO2**			
Gene symbol	**Pearson's correlation coefficient**	**P**	**Patient number**	**Gene symbol**	**Pearson's correlation coefficient**	**P**	**Patient number**
SFRP1	0.556	< 0.0001	8245	FAM136BP	-0.5519	< 0.0001	53
SAA2-SAA4	0.542	< 0.0001	481	COX7BP1	-0.4607	2.00E-04	59
KRT16P6	0.5272	< 0.0001	381	SNORD66	-0.4563	6.00E-04	53
LINC02613	0.5268	< 0.0001	381	SNORA2C	-0.4551	6.00E-04	53
KRT17P1	0.512	< 0.0001	381	SNORD99	-0.454	6.00E-04	53
CHL1-AS2	0.5093	< 0.0001	381	DHX40P1	-0.4536	6.00E-04	53
KRT16P2	0.5071	< 0.0001	564	COMMD3-BMI1	-0.4369	< 0.0001	100
CRYAB	0.5059	< 0.0001	8245	FAM138B	-0.4124	< 0.0001	171
SPECC1L-ADORA2A	0.5045	< 0.0001	139	SNORD3A	-0.407	0.0025	53
CHRDL1	0.503	< 0.0001	7950	ELOCP2	-0.4039	< 0.0001	100
RNA-sequence data							
Positive correlations with FMO2				**Negative correlations with FMO2**			
Gene symbol	**Pearson's correlation coefficient**	**P**	**Patient number**	**Gene symbol**	**Pearson's correlation coefficient**	**P**	**Patient number**
CHRDL1	0.6938	< 0.0001	4421	PAFAH1B3	-0.4036	< 0.0001	4421
SFRP1	0.6843	< 0.0001	4421				
IL33	0.6767	< 0.0001	4421				
TSHZ2	0.6742	< 0.0001	4421				
FREM1	0.6739	< 0.0001	4421				
ABCA6	0.6692	< 0.0001	4421				
BOC	0.6672	< 0.0001	4421				
LINC01140	0.6619	< 0.0001	4016				
ABCA8	0.6614	< 0.0001	4421				
ABCA9	0.6588	< 0.0001	4421				